Research Square

Preprints are preliminary reports that have not undergone peer review.
They should not be considered conclusive, used to inform clinical practice,
or referenced by the media as validated information.

Observing bright pulsating white dwarfs with PLATO: A new window into the late stages of stellar evolution

Murat Uzundag

muratuzundag.astro@gmail.com

KU Leuven

Research Article

Keywords: asteroseismology, stars, oscillations (including pulsations), stars, interiors, stars, evolution, stars, white dwarfs

Posted Date: October 10th, 2025

DOI: https://doi.org/10.21203/rs.3.rs-7408188/v1

License: This work is licensed under a Creative Commons Attribution 4.0 International License.
Read Full License

Additional Declarations: No competing interests reported.

Version of Record: A version of this preprint was published at Experimental Astronomy on June 12th, 2026. See the published version at https://doi.org/10.1007/s10686-026-10060-0.

Observing bright pulsating white dwarfs with PLATO: A new window into the late stages of stellar evolution

Murat Uzundag[1*], Alejandro H. Córsico[2,3], Nicholas Jannsen[1], Mukremin Kilic[4], Pierre Bergeron[5], Leandro G. Althaus[2,3], J. J. Hermes[6], Ingrid Pelisoli[7], Keaton J. Bell[8], Francisco C. De Gerónimo[2,3], Leila M. Calcaferro[2,3], Zsófia Bognár[9], Valérie Van Grootel[10], María E. Camisassa[11], Paulina Sowicka[12,13], Steven D. Kawaler[14], S. O. Kepler[15], Roberto Silvotti[16], Marcelo M. Miller Bertolami[2,3], Margarida Cunha[17]

[1*]Institute of Astronomy, KU Leuven, Celestijnenlaan 200D, Leuven, 3001, Belgium.

[2]Grupo de Evolución Estelar y Pulsaciones, Facultad de Ciencias Astronómicas y Geofísicas, Universidad Nacional de La Plata, Paseo del Bosque s/n, La Plata, 1900, Argentina.

[3]Instituto de Astrofísica de La Plata (IALP), CCT La Plata, CONICET-UNLP, Argentina.

[4]Homer L. Dodge Department of Physics and Astronomy, University of Oklahoma, 440 W. Brooks St., Norman, OK, 73019, USA.

[5]Département de Physique, Université de Montréal, C.P. 6128, Succ. Centre-Ville, Montréal, QC, H3C 3J7, Canada.

[6]Department of Astronomy, Boston University, 725 Commonwealth Avenue, Boston, MA, 02215, USA.

[7]Department of Physics, University of Warwick, Gibbet Hill Road, Coventry, CV4 7AL, UK.

[8]Department of Physics, CUNY Queens College, 65-30 Kissena Blvd, Flushing, NY, 11367, USA.

[9]HUN-REN Research Centre for Astronomy and Earth Sciences, Konkoly Observatory, MTA Centre of Excellence, Konkoly Thege Miklós út 15-17, Budapest, H-1121, Hungary.

[10]Space Sciences, Technologies and Astrophysics Research (STAR) Institute, Université de Liège, 19C Allée du 6 Août, Liège, B-4000, Belgium.

[11]Departament de Física, Universitat Politècnica de Catalunya, c/Esteve Terrades 5, Castelldefels, 08860, Spain.
[12]Instituto de Astrofísica de Canarias, La Laguna, E-38205, Spain.
[13]Departamento de Astrofísica, Universidad de La Laguna, La Laguna, E-38206, Spain.
[14]Department of Physics and Astronomy, Iowa State University, Ames, IA, 50011, USA.
[15]Instituto de Física, Universidade Federal do Rio Grande do Sul, Porto Alegre, 91501-970, RS, Brazil.
[16]INAF–Osservatorio Astrofisico di Torino, Strada Osservatorio 20, Pino Torinese, 10025, Italy.
[17]Instituto de Astrofísica e Ciências do Espaço, Universidade do Porto, CAUP, Rua das Estrelas, PT4150-762, Porto, Portugal.

*Corresponding author(s). E-mail(s): muratuzundag.astro@gmail.com;

Abstract

We present the scientific case for exploiting the capabilities of the PLATO mission to study bright pulsating white dwarfs across a wide spectral range, including hydrogen-deficient types (GW Vir and DBV stars) and hydrogen-rich classes (classical DAVs, pulsating extremely low-mass DA white dwarfs, and ultra-massive DA white dwarfs). PLATO's exceptional photometric precision, long-duration continuous monitoring, and extensive sky coverage promise transformative advances in white dwarf asteroseismology. Our key objectives include probing the internal structure and chemical stratification of white dwarfs, detecting secular changes in pulsation modes over extended timescales, and discovering rare or previously unknown classes of pulsators. To assess feasibility, we constructed a sample of 650 white dwarf candidates ($\boldsymbol{G \leq 17}$) identified within PLATO's Southern LOPS2 field using the PLATO complementary science catalogue combined with *Gaia* DR3, and derived atmospheric parameters through photometric modeling. This sample comprises 118 DA white dwarfs (including 23 ZZ Ceti candidates), and 41 non-DAs (including 35 DBV candidates). Simulated observations using `PlatoSim` demonstrate that PLATO will be capable of detecting white dwarf pulsation modes with amplitudes as low as ∼0.1 mma, depending on stellar magnitude, observation duration, pixel location, and the number of contributing cameras. We provide detailed detection limits and visibility forecasts for known pulsators across a representative range of these parameters. Furthermore, we emphasize strong synergies with *Gaia* astrometry, TESS photometry, and targeted spectroscopic campaigns, which together will enable robust mode identification and detailed stellar modeling. Collectively, these efforts will unlock unprecedented insights into white dwarf origins, evolution and internal physics, and the fate of their planetary systems.

Keywords: asteroseismology, stars: oscillations (including pulsations), stars: interiors, stars: evolution, stars: white dwarfs

1 Introduction

White dwarfs (WDs) are the ultimate fate of stars with initial masses below roughly 7–11 $M_{\odot}$, encompassing over 95% of all stars in the Milky Way, including our own Sun [1–4]. As such, they offer unique insights into the formation, evolution, and final stages of both stellar and planetary systems. A subset of WDs exhibit photometric variability due to various phenomena, including stellar pulsations, binarity, and transiting planetary debris [5, 6]. Stellar pulsations are particularly effective tools for probing the interiors of WDs, which undergo at least one phase of pulsational instability during their evolution. Indeed, pulsating WDs allow for asteroseismology —the study of internal structure through stellar oscillations— which has proven instrumental in refining our understanding of stellar physics [7–9].

WD pulsations are global, non-radial g (gravity)-mode oscillations with harmonic degree $\ell = 1, 2$ and periods ranging from $\sim$ 100 seconds to $\sim$ 7000 seconds and amplitudes typically below 0.4 mag [7, 9]. These oscillations are excited by different mechanisms, depending on the atmospheric composition and evolutionary stage of the star, related to partial ionization zones [$\kappa - \gamma$ mechanism; 10–14] and convection ["convective driving" mechanism; 15–17] in the outer layers.

Pulsations in WDs are extremely sensitive to the internal chemical stratification of the star, allowing for detailed asteroseismic modeling. By comparing the observed pulsation periods and period spacings with those predicted by theoretical models, we can infer key structural parameters such as effective temperature ($T_{\rm eff}$), surface gravity ($\log g$), and total stellar mass ($M_{\star}$) [e.g., 18–21]. Even more, asteroseismology enables us to probe the chemical composition of the stellar interior—including the relative abundances of oxygen (O) and carbon (C) [22–24] —as well as to estimate the extent of core crystallization [25] and the thickness of the surface hydrogen (H) or helium (He) layers [26, 27] by studying the effects of "mode trapping". Mode trapping in pulsating WDs refers to a phenomenon where certain pulsation modes are partially trapped or confined to specific regions within the star due to its internal chemical structure [28–30]. In addition, stellar rotation and magnetic fields can be investigated by examining frequency splitting in the Fourier spectra [31, 32]. Also, pulsating WDs allow us to investigate the properties of fundamental particles like axions and neutrinos and the possible variation of fundamental constants [33, 34]. Finally, pulsating massive WDs can potentially be used to study the impact of General Relativity on white dwarf structure and pulsations [35–37].

The majority of spectroscopically identified WDs possess H-rich (DA) atmospheres, with estimates generally indicating that 70–80% of WDs are H-dominated. This percentage varies with effective temperature, as shown in Figure 2 of Bédard [38], and is consistent with several spectroscopic studies, including Kepler et al. [39], O'Brien et al. [40], and Kilic et al. [41]. Pulsating DA WDs —also known as ZZ Ceti stars and DAVs—represent the most numerous class of pulsating WDs. These stars exhibit non-radial g-mode pulsations within a narrow instability strip spanning effective temperatures of $T_{\rm eff} \sim 10\,500 - 13\,000$ K and surface gravities in the range $7.5 < \log g < 9.2$. High-precision photometric observations from space missions such as *Kepler*/K2 [42, 43] and TESS [44] have been revolutionary in the study of DAVs. Indeed, the *Kepler*/K2 satellite has allowed the discovery of new DAVs, the derivation of their rotation rates, and the unexpected finding of outbursting ZZ Cetis near the red edge of the DAV instability strip, as well as the discovery of a clear dichotomy of oscillation mode-line widths in the power spectrum [31, 45–51]. The TESS mission, on the other

hand, has led to observations of numerous already known DAVs [52, 53] as well as the discovery of many new stars of this type, expanding the number of confirmed DAVs to over 500 objects [21, 54–56], and establishing them as key targets for asteroseismological investigations of WDs. TESS mission has also allowed the derivation of the rotation periods of many ZZ Ceti stars [57]. Among the H-rich pulsating WDs, we also find ELMVs, which are He-core extremely low-mass (ELM) variable WDs [58, 59]. These objects are the products of binary evolution, having lost most of their mass through interaction with a companion, and therefore never ignited He in their cores. Asteroseismology of ELMVs provides a unique window into their internal structure and evolutionary history, offering key constraints on binary mass-loss processes and the physics of compact binary systems [60–67]. TESS observations have allowed the discovery and modeling of pulsations of the ELMV star GD 278 [68], and also the study of its internal rotation [69]. Finally, among H-rich WD pulsators, there are the "hot DAVs", which are DA WDs that show photometric variability at $T_{\rm eff} \sim 30\,000$ K [70, 71], whose existence was anticipated by the theoretical calculations of [72, 73]. To this list, we must add the hypothetical "warm" ($T_{\rm eff} \sim 19\,000$ K) pulsating DA WDs, hotter than ZZ Ceti stars, which were predicted to exist in theoretical studies more than 40 yr ago [12], but that have not been detected yet [74].

The remaining ~20-30% of WDs are characterized by H-deficient atmospheres, encompassing spectral types such as PG 1159, DO, DB, and DQ [38, 75]. These stars represent a more diverse and less well-understood population compared to their H-rich counterparts. Among the H-deficient pulsators, two main classes of pulsationally unstable WDs are observed: GW Vir stars (historically also referred to as the DOV stars; see Sec. 10 in Sowicka et al. 76 for discussion) —very hot and luminous, pre-WD objects descended from PG 1159 star progenitors— and the DBV (or V777 Her) stars, which are He-atmosphere pulsators with effective temperatures near $T_{\rm eff} \sim 25\,000$ K. The evolutionary pathways that lead to H-deficient WDs remain a subject of ongoing investigation [9]. For example, DBVs may descend from PG 1159 stars after evolving through the DO phase, characterized by very hot He-rich atmospheres [3, 38]. Alternatively, they may form through the merger of two WDs. H-deficient pulsators are intrinsically rarer than DAVs, and their instability strips—defined regions in the Hertzsprung-Russell (H-R) diagram where pulsations are expected—are less well established. In many cases, the boundaries predicted by theoretical models do not coincide with those determined from observations [8, 9, 77], highlighting the need for further discoveries and detailed asteroseismic analyses to refine our understanding of these rare objects. Regarding H-deficient pulsating WDs and pre-WDs such as GW Vir and DBV stars, space missions such as *Kepler*/K2 and TESS have been highly productive, yielding discoveries of new pulsating stars, new periods in known pulsating stars, and confirmation of previously detected periods from ground-based observations [78–84]. In many cases, it has been possible to infer the total mass, internal chemical layering, and rotation rates using asteroseismic techniques such as asymptotic period spacing, period-to-period fits and rotational splitting. Also, it has been possible to infer the asteroseismic distances and compare them with the *Gaia* distances. Another interesting aspect of seismological modeling of these stars is the prediction of the rate of change of their periods, which can be compared with the observed rates [for example, see 82].

In this paper, we propose a coordinated effort to utilize data from upcoming space missions—particularly PLATO (PLAnetary Transits and Oscillations of stars) —along with

ground-based follow-up to conduct asteroseismological analyses of pulsating WDs across all subtypes. Such efforts will significantly advance our understanding of stellar remnants and the fate of planetary systems.

2 The Complementary Science Program

To harness the full scientific capabilities of the PLATO mission beyond its core science objectives, the PLATO Complementary Science (CS) Program—also referred to as PLATO-CS—has been established [85, 86]. This initiative is designed to support diverse scientific investigations by allocating 8% of PLATO's telemetry budget to non-core science cases through a dedicated Guest Observer (GO) program [87]. These open, competitive calls will allow the broader astronomical community to propose studies of specific astrophysical targets not covered by the core mission. PLATO-CS plays a pivotal role in shaping and preparing these GO calls, ensuring high-impact science opportunities are made available. This 8% telemetry allocation enables the monitoring of thousands to tens of thousands of strategically selected objects, including rare and compact stars such as WDs and hot subdwarfs. In this paper, we present the science cases we intend to pursue within the GO framework, highlighting the unique potential of PLATO data to advance our understanding of compact pulsators and related phenomena.

3 Science Goals

The interior properties of WDs encode the history of the star's prior evolution [3, 4, 88]. WD asteroseismology not only reveals the current internal structure of WDs, but also constrains the physical processes that shaped their progenitors, such as core growth during He burning, thermal pulses on the asymptotic giant branch (AGB), and late thermal pulses [7–9, 89]. For example, DBVs can help trace the evolution of He-rich post-AGB stars, while GW Vir stars may retain signatures of very late thermal pulse events. To fully exploit this potential, it is crucial to detect a large number of pulsation modes. The more modes we observe, the more accurately we can constrain the internal structure and test evolutionary models. However, many WDs observed so far have shown only a few dominant pulsation periods, often due to observational limitations such as cadence, duration, and noise level.

PLATO's long-duration, high-precision, and high-cadence observations offer a transformative opportunity to expand the mode detection capabilities for WD asteroseismology. By enabling continuous, high signal-to-noise monitoring of bright pulsators, PLATO will allow us to:

- Track temporal evolution of pulsation frequencies and amplitudes, probing processes such as cooling, mode trapping, and rotational splitting;
- Identify rotational multiplets to directly measure internal rotation rates;
- Search for new or rare classes of pulsators, including ultra-massive and extremely low mass WDs;
- Search for and identify pulsations in candidate objects such as hot DAVs, for which the origin of variability remains uncertain. Expanding the sample of confirmed pulsators in this category is crucial for refining pulsation theory and testing models of WD formation and evolution;

- Characterize the crystallization process in ultra-massive pulsating WDs through the detection of the period spacing.

These goals will be addressed through a coordinated GO program, focusing on a well-curated sample of known and candidate pulsators. PLATO's long-baseline observations and high cadence will be essential for resolving low-amplitude and closely spaced pulsation modes. The goals will be further enhanced through synergies with *Gaia* astrometry, TESS light curves, and ground-based spectroscopic follow-up, which together provide independent constraints on stellar parameters and mode identification.

In summary, PLATO will significantly extend the frontiers of WD asteroseismology, offering an unprecedented view into the physics of stellar remnants and the evolutionary history of low- and intermediate-mass stars.

3.1 DAV Stars

DAVs (ZZ Ceti stars) are the most common class of WD pulsators, typically found at $T_{\rm eff} \sim 12,000$ K. Despite their ubiquity, several open questions remain regarding their instability strip boundaries, internal structure, and evolutionary histories. With its high precision and extended time coverage, PLATO offers a transformative opportunity to advance DAV studies by:

- Expanding the sample of hot (blue-edge) DAVs, which are currently underrepresented, to refine instability strip boundaries and test driving mechanisms,
- Searching for temporary overall brightness changes coupled with the pulsations, such as outbursts,
- Discovering many new ZZ Ceti stars, which could potentially allow confirmation of the existence of a mass range of the H envelope in DA WDs, as past analyses have suggested,
- Searching for elusive warm DAVs ($T_{\rm eff}$ ~19,000 K) with very thin H layers, predicted to be unstable to *g* modes, but yet to be observed,
- Resolving rotational multiplets to probe internal rotation and angular momentum loss,
- Detecting long-term amplitude and frequency modulations to investigate mode coupling, convection, non-linear effects, and possible evolutionary changes,
- Enabling detailed asteroseismology to constrain crystallization processes, core composition, and phase transitions,
- Identifying and characterizing polluted DAVs to explore accretion geometry and link pulsations to external planetary debris.

3.2 ELMV Stars

ELMVs (pulsating low-mass and extremely low-mass WDs) are He-core WDs formed in compact binary systems after undergoing intense mass loss. They exhibit long-period *g*-mode pulsations that make them valuable asteroseismic targets. With PLATO, we aim to:

- Detect new ELMV pulsators suitable for asteroseismology,
- Constrain H envelope thickness and mass-loss history,
- Measure surface rotation through resolved multiplets.

3.3 Pulsating Ultra-massive DA WDs

UM (ultra-massive) DA WDs are characterized by stellar masses $M_\star \gtrsim 1.05\,M_\odot$. Pulsating UM DA WDs constitute an excellent opportunity for studying a wide variety of fundamental processes, including the final stages of stellar evolution, the progenitors of type Ia supernovae, the outcomes of WD mergers, the physics of the super-asymptotic giant branch (SAGB), and the effects of core crystallization. These stars are also often associated with strong magnetic fields. Different evolutionary scenarios are proposed for the formation of UM WDs: (1) isolated evolution of intermediate-mass stars, for which C ignites in their interior, leading to a ONe-core UM WD, (2) isolated evolution for which the presence of weak winds or fast rotation could avoid C-ignition, resulting in a CO-core UM WDs, and (3) post-merger evolution of binary WDs, leading to ONe- and potentially CO-core compositions. The internal composition and origin of UM WDs remain uncertain, and pulsations offer one of the few direct methods (if not the only one) to probe their cores. With PLATO's precision photometry, we aim to:

- Identify and characterize new pulsating UM DAVs,
- Search for UM DAQV stars, like WD J0551+4135[1], which challenge WD formation theories;
- Measure period spacing patterns to test core composition and crystallization theory,
- Search for mode trapping and rotational splitting to constrain envelope layering and angular momentum,
- Distinguish between single-evolution and merger-origin scenarios through detailed asteroseismic modeling.

3.4 GW Vir Stars

GW Vir stars, also known as PG 1159 pulsators, are hot, hydrogen-deficient post-AGB stars in a brief but crucial phase of stellar evolution. The classification of GW Vir stars also includes the pulsating Wolf-Rayet central stars of planetary nebula (WC) and early-WC (WCE) stars because they share the pulsation properties of pulsating PG 1159 stars [91]. They exhibit non-radial g-mode pulsations that provide insight into their internal structure and evolutionary state. Despite being located within the theoretical instability strip, only about 36-50% of these stars are observed to pulsate [76, 79, 81], indicating an incomplete understanding of the driving mechanisms and instability boundaries [91]. The prototypical and most studied object of this class is PG 1159-035 (GW Vir). Results from the most recent asteroseismological analyses of this star are disturbing, since the seismological model (which accurately reproduces the observed periods) lies outside the instability domain of these stars [82, 92]. Also, the observed rates of period changes [93] are ten times smaller than those predicted by the seismological model. In addition, the rates of period change predicted by the best-fit model are positive for all modes, and thus they do not agree with the observed positive and negative values. Reconciling theoretical predictions with observations remains a challenge.

PLATO's precise and long-duration photometry will significantly advance our knowledge of these stars by enabling the following:

[1] This is the only pulsating DAQ WD with a C and H atmosphere known [90]

- Expanding the sample size to better constrain the efficiency and boundaries of the GW Vir instability strip,
- Searching for correlations between surface abundances and pulsation occurrence, in order to understand the strip's impurity and test proposed excitation/damping mechanisms,
- Monitoring secular period changes caused by rapid cooling and contraction. GW Vir stars evolve quickly, and PLATO's long-term coverage will enable us to determine these evolutionary changes on timescales of just a few years.

3.5 DBV Stars

DBV stars are He-atmosphere WDs pulsating at $T_{\rm eff} \sim 25,000$ K. Increasing the number of known DBVs is critical for constraining their poorly understood evolutionary origins, particularly the role of convective dilution versus alternative channels like binary mergers. PLATO's high-precision photometry and long-time baselines will enable us to:

- Expand the population of DBVs for asteroseismic modeling, to probe internal structure and test evolutionary scenarios,
- Search for pulsating UM DBVs. Being much hotter and less crystallized than UM DAVs, if they exist, they would allow probing deeper regions with the g-mode pulsations, potentially providing information on the structure and chemical composition of the core,
- Identify stable pulsators near the blue edge to measure WD cooling rates and constrain plasmon neutrino and axion emission from rates of period changes,
- Monitor period changes and amplitude modulations to investigate nonlinear mode interactions and long-term evolution,
- Empirically refine the location and extent of the DBV instability strip to calibrate convective efficiency and improve diffusion models relevant for planetary debris analysis,
- Searching for outbursts in cool DBVs —there are hints that outbursts could have been observed in at least one DBV in the past [the "forte" or "sforzando" event observed in GD 358; 94–96].

4 Sample selection

As part of a larger simulation study for the 'Pulsating Stars' work package of the PLATO-CS, [97] generated a PLATO asteroseismic mock catalogue (MOCKA). An important delivery of MOCKA is a *Gaia* DR3 source catalogue of stars brighter than $G < 17$ within the first Southern long-duration observational phase [LOPS2; 98]. With six co-pointing 'normal' cameras (N-CAMs), situated in four camera groups each with an opening angle of 9.2° relative to the platform pointing, each PLATO pointing field display a characteristic geometric feature. This is also known as the N-CAM visibility flower, and is a result of the partial overlapping number of N-CAMs, counting $n_{\rm CAM} \in \{6, 12, 18, 24\}$ (which will be shown in Sect. 8).

The PLATO–LOPS2 *Gaia* DR3 (from hereon PLATO-CS) catalog contains almost eight million sources in the magnitude range $2 \leq G \leq 17$. To identify white dwarf (WD) candidates within this sample, we cross-matched PLATO-CS with the catalog from Gentile Fusillo et al. [99] of high-confidence WDs based on *Gaia* EDR3, as well as the catalog of ELM WD candidates from Pelisoli and Vos [100]. Through this combined approach, we identified an initial sample of 649 WD candidates within the LOPS2 region. Figure 1 shows the H-R diagram

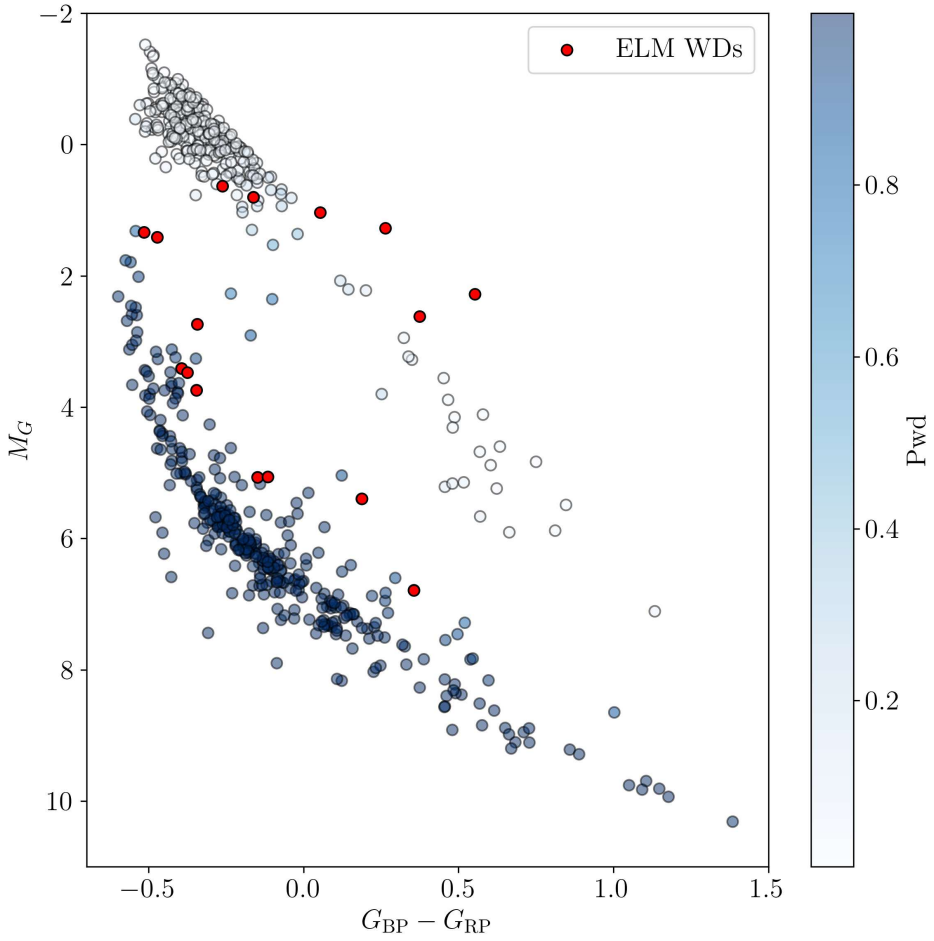


Fig. 1 H-R diagram of white dwarf candidates identified in the PLATO-CS input catalog [97]. The color bar indicates the WD probability from Gentile Fusillo et al. [99]. Extremely low-mass (ELM) WD candidates, selected from the PLATO-CS catalog and cross-matched with the sample of Pelisoli and Vos [100], are shown in red.

of our initial WD candidates identified in the PLATO-CS input catalog. Each candidate was assigned a WD probability following Gentile Fusillo et al. [99], with increasing probability the darker the shade of blue.

5 Photometric model atmosphere analysis

To determine the fundamental atmospheric parameters of our white dwarf sample, we use the photometric method [101], which relies on multi-band photometry combined with precise astrometric data from *Gaia* DR3.

We use broad-band photometry from Skymapper (*uvgriz*, available for 99% of the sample) and Pan-STARRS (*grizy*, availabe for 23% of the sample), along with *Gaia* parallaxes, to constrain both the effective temperature and the solid angle, $\pi(R/D)^2$, of each star. Given the accurate distances from *Gaia*, we directly estimate the stellar radii, which are then combined with white dwarf evolutionary models to derive the stellar masses. For a small sample of stars, where the Skymapper or Pan-STARRS photometry is unavailable or contaminated by a neighboring source, we instead rely on the *Gaia* G, $G_{\rm BP}$, and $G_{\rm RP}$ photometry.

The observed magnitudes are first converted into average fluxes, which are then compared to synthetic fluxes generated from model atmospheres corresponding to various temperatures and chemical compositions. We minimize the χ^2 difference between observed and model fluxes across all bandpasses using the Levenberg–Marquardt nonlinear least-squares algorithm [102], yielding the best-fit atmospheric parameters. Uncertainties on the fitted parameters are derived from the covariance matrix of the fitting routine. For parameters calculated from these fits, such as mass and radius, uncertainties are propagated in quadrature from the input measurement errors.

Our analysis utilizes pure H and mixed H/He models with log (H/He) = −5 as described in Bergeron et al. [101]. Only 79 of our targets have spectra available in the Montreal White Dwarf Database [103], though a larger number has spectral types provided in the literature. For the ones without follow-up spectroscopy, we provide both pure H and mixed H/He model fits as representative solutions. We adopt the evolutionary models of Bédard et al. [104], which assume carbon-oxygen cores with helium and hydrogen envelope layer masses of q(He) = 10^{-2}, and q(H) = 10^{-4} (for H-atmosphere white dwarfs) or 10^{-10} (for He-atmosphere white dwarfs). These assumptions are representative of DA and DB white dwarfs, respectively.

As an example, Figure 2 shows our model fits to one of the pulsating ZZ Ceti stars known in the PLATO field, WDJ053306.78−560353.38 (HE 0532−5605). The top panel shows the Skymapper *uvgriz* photometry (error bars) along with the predicted fluxes from the best-fitting pure H (filled dots) and pure He (open circles) atmosphere models. The labels in the same panel give the name, *Gaia* source ID, and the photometry used in the fitting. The photometry clearly favors the pure H solution, where a Balmer decrement is visible between the *uv* and *g* bands. The middle panel shows the predicted spectrum based on the pure hydrogen solution (red line), along with the observed Hα line. This is not a fit to the line profile, we simply over-plot the predicted hydrogen line from the photometric fit. The bottom panel shows a broader spectral range. The photometric fit provides an excellent match to the Hα line for this white dwarf, confirming that this is a pure hydrogen atmosphere white dwarf with $T_{\rm eff}$ = 10 915 ± 121 K and M = 0.820 ± 0.012 $M_{\odot}$.

Tables A1 and A2 in the Appendix present the white dwarf parameters derived in this work. These tables compile the targets fitted with pure-H (He/H = 0) and He-rich atmospheres with trace amounts of hydrogen (log H/He = –5). Each table lists *Gaia* DR3 data (WD name, *Gaia* source ID, RA, Dec, probability of being a white dwarf, and G magnitude), PLATO Input Catalog (PIC) information (P magnitude and number of cameras), and the physical parameters ($T_{\rm eff}$, log g, and mass) derived from our photometric fits. There are 118 DA stars in total, listed in Table A1, with a subset (23) falling within the ZZ Ceti instability strip; these objects will be prioritized for future follow-up studies (see Section 6.1). In addition, 6 stars classified as DB, DBA, DBAZ and 35 stars are DBV candidates (see Section 6.2) are included,

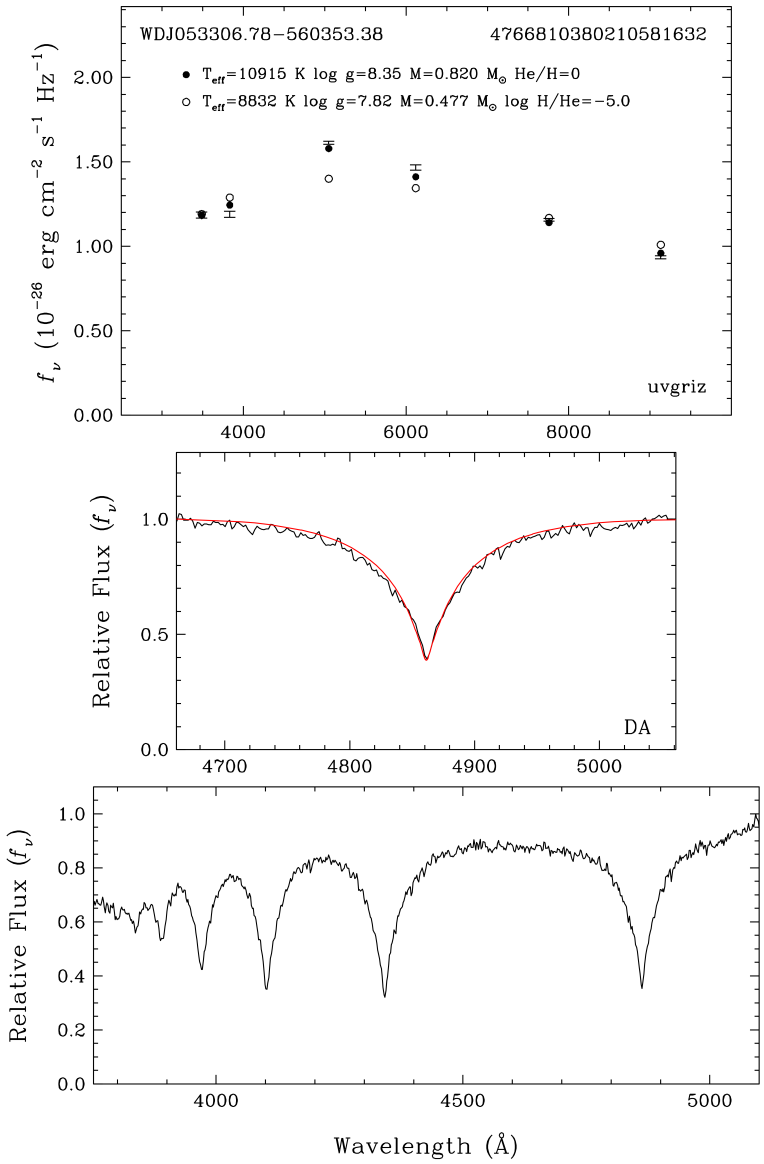


Fig. 2 Model fits to the DA white dwarf WDJ053306.78−560353.38 (HE 0532−5605), which is a previously known ZZ Ceti pulsator in the PLATO field. The top panel shows the best-fitting pure H (filled dots) and pure He (open circles) atmosphere white dwarf models to the Skymapper photometry (error bars). This panel also includes the name and the *Gaia* Source ID, and the photometry used in the fitting. The middle panel shows the predicted spectrum (red line) based on the pure-H solution, overplotted on the observed spectrum (black line). The bottom panel presents the same comparison over a broader wavelength range.

with mixed atmosphere model solutions provided in Table A2. The broader sample includes stars of other spectral types (e.g., DZ, DC, very hot WDs), but because these preliminary fits are not sufficiently robust — and in some cases may involve misclassifications such as hot subdwarfs — they are not published here. These preliminary estimates will instead remain available for internal use (e.g., target selection and follow-up planning) but are deliberately excluded from the paper to avoid confusion and ensure reliability of the published parameters.

While the Gaia DR3 XP spectra and the synthetic photometry from the [105] catalog offer an important complementary resource for WD classification and parameter estimation, our analysis is based on an independent photometric fitting approach. Although the machine-learning classifications from XP photometry are generally reliable for DA white dwarfs, we noted inconsistencies for other spectral types, particularly for DB, DQ, and magnetic white dwarfs based on comparisons with follow-up spectroscopy. Since the method presented in [105] also relies on photometric fitting techniques similar to ours, and adopts pure-He models for DBs, we opted for a more conservative approach. Our analysis includes both pure-H and mixed H/He models, which are more appropriate for DB white dwarfs, especially given that many ($\sim 75\%$) DBs in the solar neighborhood also show trace amounts of H [DBA spectral type, 41, 106]. This distinction is crucial, as our mixed-atmosphere models yield cooler temperatures for several DBV candidates, affecting their classification within the instability strip.

6 Pulsating WD candidates in the LOPS2

6.1 DA instability strip

Figure 3 shows the ZZ Ceti instability strip for PLATO WDs (open circles) under the assumption of pure H atmospheres. Here we exclude spectroscopically confirmed non-DAs and magnetic white dwarfs. The blue and red lines show the empirical boundaries of the ZZ Ceti instability strip from Vincent et al. [107]. Blue dots mark the three previously known DAV pulsators, whereas the green dots mark the ZZ Ceti candidates that fall near or within the instability strip. We inspected the photometric spectral energy distributions of each candidate, and rejected the sources where the photometry clearly favors the He-atmosphere solution. At $T_{\rm eff} \sim 11\,000$ K, DA WDs show a clear Balmer decrement, which is typically visible between the *uv* and *g* filters (see Figure 2). We rejected 10 of the candidates as likely He-atmosphere objects; those are the open circles within the instability strip.

In total, we identify 23 ZZ Ceti candidates, where the spectral energy distributions are consistent with pure H atmospheres. Seven of these are spectroscopically confirmed to be DA WDs, including three pulsators. The known ZZ Ceti stars include the average mass WDJ045527.27−625844.61 with $T_{\rm eff} = 11\,106 \pm 115$ K and $M = 0.514 \pm 0.009\ M_{\odot}$, the massive WDJ053306.78−560353.38 with $T_{\rm eff} = 10\,915 \pm 121$ K and $M = 0.820 \pm 0.012\ M_{\odot}$, and the apparently low-mass WDJ071114.41−251815.05 with $T_{\rm eff} = 10\,677 \pm 40$ K and $M = 0.251 \pm 0.001\ M_{\odot}$.

We also identify the DA white dwarf WDJ053203.91−653609.91 with $T_{\rm eff} = 11,330 \pm 250$ K and $M = 0.549 \pm 0.02\ M\odot$, and the candidate ZZ Ceti WDJ060052.91−463041.11, whose atmospheric parameters vary between two solutions: a low-temperature, low-mass fit with $T_{\rm eff} = 9857 \pm 100$ K and $M = 0.261 \pm 0.004 M_{\odot}$, and a higher-temperature solution with $T_{\rm eff} = 13,210 \pm 162$ K and $M = 0.331 \pm 0.006 M_{\odot}$.

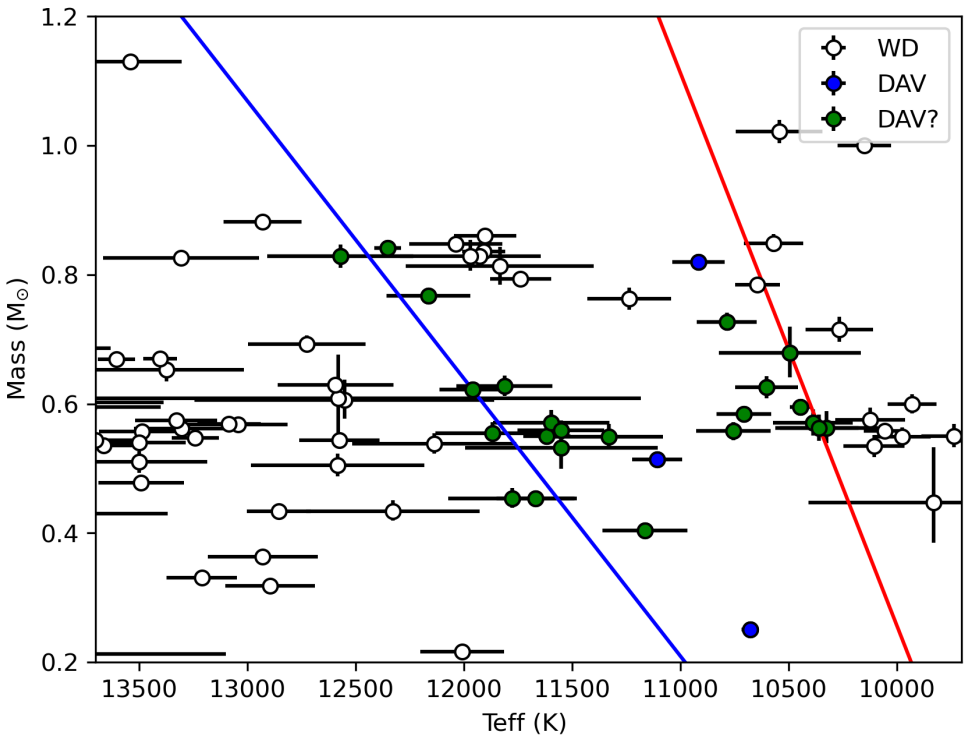


Fig. 3 Masses and effective temperatures for the PLATO WD sample assuming pure H atmospheres (open circles). The blue and red lines show the empirical boundaries of the ZZ Ceti instability strip from Vincent et al. [107]. Blue dots mark the three known ZZ Ceti stars in the sample, whereas the green dots mark the DAV candidates that fall near or within the instability strip and also have photometric spectral energy distributions consistent with DA white dwarfs.

WDJ045527.27−625844.61 shows 4 pulsation modes in TESS with periods ranging from 126.8 to 320.8 s. Performing asteroseismology based on these four modes, Romero et al. [54] derive a mass of 0.542 $M_{\odot}$, which is similar to the mass that we obtain from its spectral energy distribution and *Gaia* parallax. Similarly, WDJ053203.91−653609.91 exhibits pulsations with periods of 275.49 s and 411.28 s, and has an effective temperature of 12, 390 K and a mass of approximately $0.66M_{\odot}$ [54]. WDJ060052.91−463041.11 shows a pulsation period of 268.45 s but presents a degenerate solution in its atmospheric parameters, with one fit yielding $T_{\rm eff} \approx 12,150$ K and $M \approx 0.493M_{\odot}$, and an alternative cooler solution at $T_{\rm eff} \approx 9,350$ K with $M \approx 0.303M_{\odot}$ [54]. WDJ053306.78−560353.38 shows 8 modes ranging from 522 to 724 s [108], which is consistent with a pulsating massive DAV. On the other hand, based on a single detected mode at 278 s in TESS data, Romero et al. [54] derive a mass of 0.632 $M_{\odot}$ for WDJ071114.41−251815.05, which is inconsistent with our mass estimate. Note that Gentile Fusillo et al. [99] also find a mass of $\approx$ 0.3 $M_{\odot}$ based on *Gaia* photometry and astrometry for the same star. WDJ071114.41−251815.05 is clearly over-luminous. The discrepancy between the asteroseismological and photometric mass estimates can be resolved if this is a

Table 1 DAV Candidates in the PLATO field.

Name	*Gaia* Source ID	$T_{\rm eff}$ (K)	Mass ($M_\odot$)
WDJ041930.81−352046.73	4870090943381248128	10602	0.626
WDJ045359.85−432247.75	4811871287295222016	11162	0.404
WDJ045405.87−342505.71	4873109308958466432	11960	0.622
WDJ045551.33−705541.81	4654695103690489856	10324	0.563
WDJ052518.96−302018.13	2905372374461903488	11616	0.550
WDJ052548.76−671611.58	4658691072554066560	10493	0.679
WDJ052912.10−430334.49	4805782462481529600	11669	0.454
WDJ053100.49−455801.14	4799224635833122304	10387	0.571
WDJ053203.91−653609.91	4660769493122896128	11330	0.549
WDJ053939.69−664157.85	4659528969150132096	11868	0.555
WDJ054458.33−401940.13	4805139866655106944	11596	0.571
WDJ055428.05−402555.11	4804209684114310784	12570	0.829
WDJ060013.07−545516.04	5500308124837433984	10785	0.727
WDJ064802.46−483039.16	5551402808137892864	11551	0.559
WDJ071051.17−342107.14	5602672550010235008	10707	0.584
WDJ071751.88−282928.84	5606764386835758720	10444	0.595
WDJ072717.48−332838.16	5592485716514387584	11775	0.454
WDJ073338.28−281623.17	5611744006283630720	12351	0.841
WDJ074613.81−302550.93	5598661329740179712	10754	0.558
WDJ075643.91−545348.89	5296195267296378112	11549	0.532
WDJ083246.58−574125.49	5315128548292806656	11812	0.628
WDJ083759.16−501745.76	5322090003089341440	12163	0.767
WDJ084215.26−555628.51	5316824544982104960	10358	0.563

binary system, where the extra light from the companion results in an inflated radius estimate and a lower mass. Note that the 278 s mode is significantly shorter than the typical pulsation modes seen in ELM WDs [58, 59]. Hence, WDJ071114.41−251815.05 likely represents a pulsating DA with a WD companion. We provide the list of the remaining 23 ZZ Ceti candidates in Table 1; 19 of these lack spectroscopy. We plan on obtaining follow-up spectroscopy to confirm their nature and their suitability for PLATO observations.

6.2 DB instability strip

Figure 4 displays the location of PLATO DB white dwarfs modeled under the assumption of He-rich atmospheres (with traces of hydrogen) in the $T_{\rm eff}$–surface gravity plane. As for the DA analysis, we removed spectroscopically confirmed magnetic WDs. The blue and red dashed lines trace the empirical boundaries of the DB instability strip, which we extend using the work of Córsico et al. [9] and Vanderbosch et al. [77]. Blue points mark stars that fall within or near the instability strip. The only currently known DBV in the PLATO field, WDJ052330.80=472219.55, is highlighted with a red dot; its location within the strip provides an important anchor point for our analysis. In total, we identify 35 DBV candidates, which are listed in Table 2. These stars have effective temperatures ranging from $\sim$ 17 000 K to 32 500 K and span a broad mass range of about $0.40 - 0.71 M_\odot$. Unfortunately, the photometric spectral energy distributions do not allow us to distinguish between DA and DB white dwarfs at these temperatures. Hence, follow-up spectroscopy is required to confirm DB white dwarfs in this sample.

The only confirmed DBV in our sample, WDJ052330.80−472219.55 (EC 05221−4725), was identified as a pulsating DB white dwarf by Kilkenny et al. [109], who reported clear variability with a dominant period near 15 minutes. Their time-series photometry revealed a

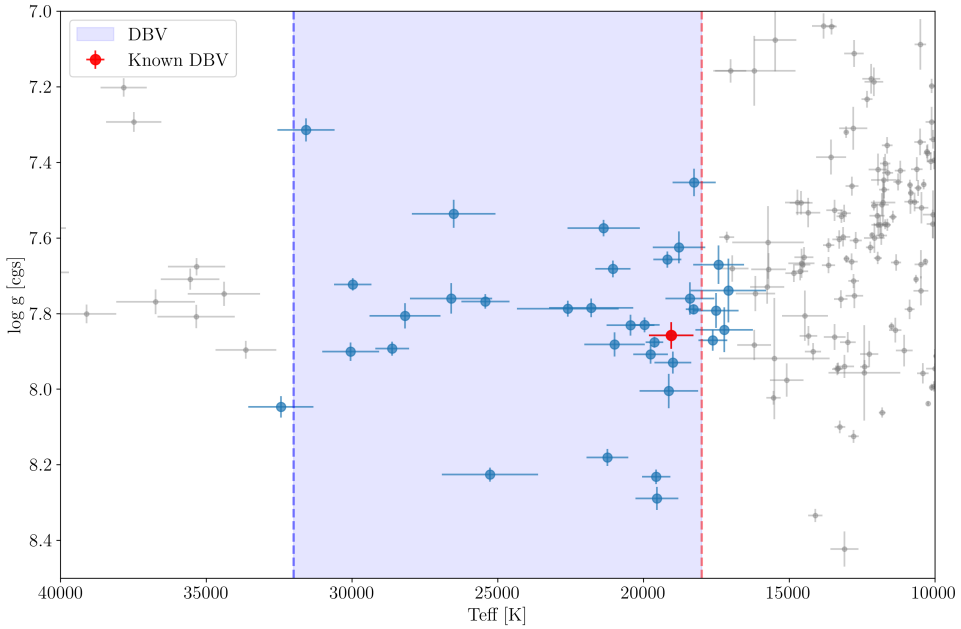


Fig. 4 Location of the PLATO white dwarf sample in the effective temperature–surface gravity plane, modeled under the assumption of He-rich atmospheres. The blue and red dashed lines indicate the extended empirical boundaries of the DB instability strip based on Córsico et al. [9], Vanderbosch et al. [77]. Blue points highlight stars located within or close to the strip. The known DBV WDJ052330.80−472219.55 is marked with a red dot.

persistent frequency around ∼890 s and additional peaks near ∼810 s, alongside evidence for amplitude modulation and beating effects, suggesting a complex pulsation spectrum worthy of further study. Upcoming long-baseline, high-precision light curves from PLATO will be extremely valuable for resolving its rich frequency spectrum and assessing mode stability.

7 Other Types of Variable White Dwarfs in the LOPS2

Beyond pulsating white dwarfs, we also investigated other types of variable white dwarfs in our sample. Using the `TESS-Localizer` tool [110], we extracted and classified light curves from TESS-observed targets, identifying 24 variable white dwarfs. These variables exhibit a wide range of behaviors, including short-period binary systems, eclipsing binaries, spotted white dwarfs, candidates for ELMVs, and potential cataclysmic variables. The variability observed is often attributed to rotational modulation or binary interactions, with periods ranging from less than one hour to several tens of hours. Approximately 15 of these variable white dwarfs coincide with targets studied in recent works [e.g., 111, 112], which focus on magnetic white dwarfs and other notable variable types. Within this sample, we confirmed three cataclysmic variables, namely TIC 364266095 [Var Ret2005, 113], TIC 172467837 [PU CMa, 114, 115], and TIC 25133286 [VW Hyi, 116]. We identified two short-period binaries hosting extremely low-mass white dwarfs: TIC 278861557 (P_{orb} = 3.12,hr; J0642−5605)

Table 2 DBV Candidates in the PLATO field.

Name	*Gaia* source ID	$T_{\rm eff}$ (K)	Mass ($M_\odot$)
WDJ041724.58-673236.77	4668242152077665024	17419	0.428
WDJ042610.85-465847.47	4789144175789941888	20442	0.51
WDJ043151.06-532929.85	4780712394777586560	28181	0.514
WDJ050510.82-613924.40	4760710942535282560	21235	0.709
WDJ053423.94-381444.86	4808986478021189120	26509	0.401
WDJ054007.06-651807.95	4660085867450146560	17084	0.458
WDJ054657.41-305153.89	2903068214703934848	25266	0.742
WDJ055635.50-561006.57	4767225652008399104	19561	0.739
WDJ060612.38-723414.20	5266145236552677632	18259	0.348
WDJ060740.96-285302.51	2897810350100517504	18283	0.484
WDJ061109.12-703921.89	5278615205944625664	26597	0.49
WDJ061238.45-325357.56	2892795821161588736	19180	0.427
WDJ061524.39-384823.63	5574654180530308736	25422	0.491
WDJ061856.82-372607.54	5575200775248718976	22594	0.493
WDJ062000.90-233500.19	2936643760765256576	21047	0.442
WDJ063814.10-694335.39	5278903110486861312	32439	0.646
WDJ063845.14-470141.00	5552665081846145024	17512	0.484
WDJ064648.90-525349.76	5498647381243346176	18988	0.558
WDJ064747.51-270813.49	2919284671187233280	28620	0.557
WDJ065112.06-440937.57	5562002134589548032	18778	0.413
WDJ065703.65-433414.37	5559127976835354624	18403	0.471
WDJ065957.09-291701.35	5608058473357824128	21363	0.4
WDJ070918.12-302728.87	5604654870693369984	29970	0.481
WDJ073920.28-262915.39	5613838438495596032	19624	0.53
WDJ074250.12-544920.12	5488182813687216000	19127	0.6
WDJ074521.91-432803.38	5532479697634251776	19536	0.775
WDJ081612.57-402513.53	5539643909237818880	21792	0.49
WDJ081827.11-460309.83	5519761028164909568	17228	0.508
WDJ082109.21-500114.40	5514870018179554560	31577	0.343
WDJ083341.91-655530.74	5272852979034659072	19752	0.547
WDJ083942.55-535949.14	5317871245692348032	20988	0.536
WDJ085424.48-491724.58	5328333889104483712	30045	0.564
WDJ041909.91-535045.31	4779379172505736832	17617	0.524
WDJ042211.36-474142.02	4788896304637763072	19960	0.508
WDJ052330.80-472219.55	4797409582653745152	19045	0.52

[117] and TIC 310478036 ($P_{\rm orb}$ = 2.32,hr; SDSS,J083417.21−652423.2) [118]. In addition, TIC 279321596 exhibits spot modulation, while TIC 430591603 is a candidate ELMV white dwarf warranting further follow-up observations.

Finally, thanks to its blue bandpass and fast cadence, PLATO could uncover new transiting systems among white dwarfs if monitored. Using Gaia EDR3 data [99], Eschen et al. [119] identified two promising targets in the LOPS2 field: RXJ0623.2−3741 (TIC 237397195), a metal-polluted white dwarf and strong planet-host candidate [120], and ϵ Ret B (TIC 684987240), the white dwarf companion to a known planet-hosting K subgiant [121, 122]. The authors emphasize that white dwarfs in LOPS2 can achieve photometric precision comparable to PIC stars, and that deeper transits around white dwarfs make even fainter targets suitable for exoplanet detection.

8 Simulations

We use the PLATO camera simulator [PlatoSim, 123] to assess the feasibility to use PLATO for WD asteroseismology. As discussed in Sect. 4, light curves of WD pulsators were simulated as part of the MOCKA catalogue [97]. While the analysis of MOCKA's simulated dataset focused on main sequence g-mode pulsators, the simulations showed principally that PLATO can detect pulsations with amplitudes < 0.1 ppt and resolve closely spaced modes even at a 600s cadence while using input templates based on *Kepler*, TESS, and ground-based light curves.

As part of the MOCKA catalogue, 30 pulsating WD stars from the PLATO-CS input catalogue (c.f. Fig. 1) were simulated: 10 DAV with pulsation modes extracted from *Kepler* observations, and 10 DAV, 5 DBV, and 5 GW Vir stars with pulsation modes extracted from TESS observations. These 30 targets were selected based on being the richest pulsators, i.e. with the largest number of pulsation periods detected. While the pulsation modes were used to construct the injected template light curves, each pulsator was further simulated for ten different PLATO-CS catalogue stars across the four N-CAM visibilities. In the initial work by Jannsen et al. [123], 10 pulsating white dwarf stars from the PLATO-CS input catalogue were simulated. As an extension to this effort, we additionally selected and simulated ten more stars — thus increasing the sample to 20 in total — to ensure that five stars are observed by 6, 12, 18, and 24 co-pointing N-CAMs. Thus, besides the N-CAM visibility, the 30×20 stars simulated were selected to cover a wide parameter space in P-band magnitude (from $\sim$ 12 to $\sim$ 17 mag), in random and systematic noise (unique for each of the 20 stars' location in the focal plane array), and levels of stellar contamination from nearby stars. Thus, all in all, realistically representing future observations. Figure 5 shows the LOPS2 overplotted with the WD candidates from the PLATO-CS input catalogue (color coded after PLATO magnitude). The 20 WD candidates used to generate all simulated light curves of this paper are illustrated with pink circles.

In order to gain some basic insight to what kind of data quality PLATO will provide for pulsating WDs, we first investigate the underlying noise budget in the time domain. For our 30 mock stars, we investigate the noise-to-signal ratio (NSR) derived from 24-h PlatoSim light curves as function of P-band magnitude and co-pointing cameras. We illustrate this in Fig. 6 where each WD candidate has a unique color-coding, while DAV, DBV, and GW Vir stars are marked with circles, squares, and stars, respectively. To first order, a given pulsation mode can only be detected if the pulsation amplitude is above (with a few orders of magnitude) the NSR level. As a reference we provide six NSR median estimates, derived from MOCKA light curves. As an example, it is evident that for $n_{\rm CAM} = 24$ and $P \leq 12$, almost all pulsations modes will be detectable (notably those of DAV star EPIC 229227292 and the GW Vir star TIC 035062562 i.e. GW Vir itself). Meanwhile for $n_{\rm CAM} = 6$ and $P \geq 16$, only a fraction of the modes are expected to be detected. While this is indicative of the mode occurrence rates for WD pulsators, a thorough frequency analysis is needed to access the underlying potential PLATO will provide WD research, which is the topic of the following discussion.

Considering now our simulated PLATO light curves, we overall find a good agreement in the pulsation mode detectability derived from amplitude spectra as compared to the (above mentioned) estimates in the time domain. In Appendix B, we present as a show-case the amplitude spectra for three representative pulsating WDs simulated with PlatoSim: the DAV TIC422526868 (G29-38, Fig. B1), the DBV TIC219074038 (GD358, Fig. B2), and the GW

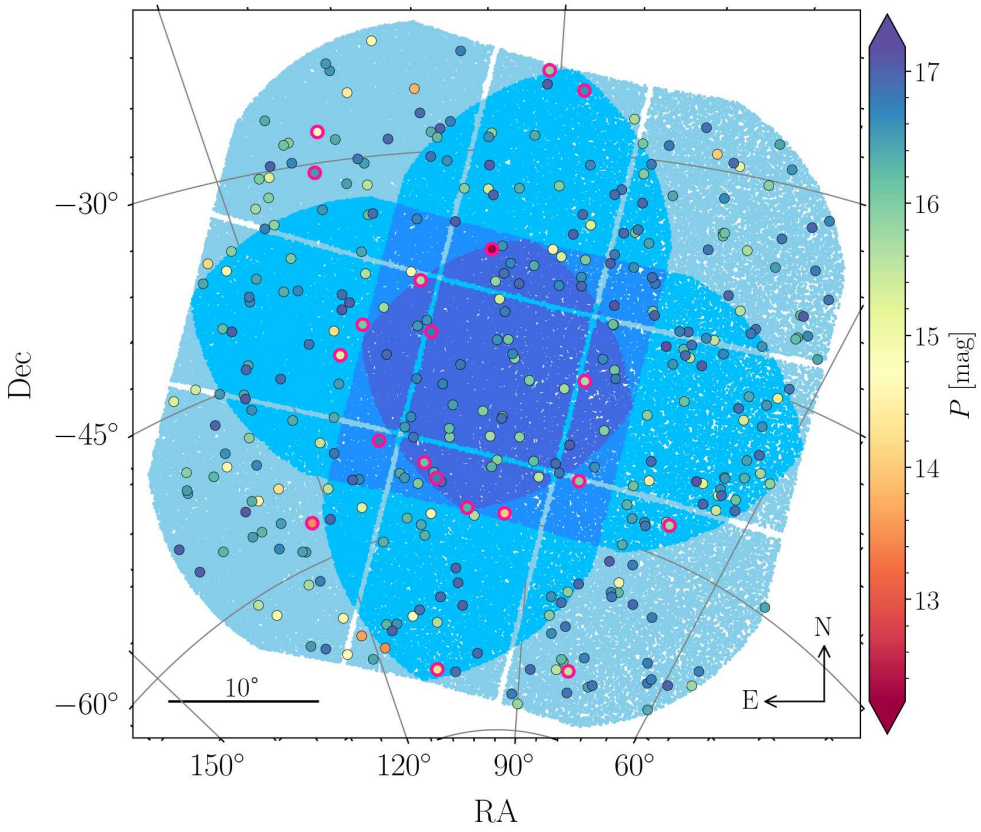


Fig. 5 The first PLATO pointing field in the South, LOPS2, shown in equatorial coordinates. The increasing darker shade of blue illustrates the N-CAM overlap of $n_{\rm CAM} \in \{6, 12, 18, 24\}$, respectively. The color coded circles (according to the PLATO N-CAM passband magnitude, P) shows the WD candidates from Fig. 1, while the pink circles show the 20 WD stars from the PLATO-CS catalogue used for simulations in this paper. This figure has been adapted from [97].

Vir star TIC035062562 (PG1159-035, Fig. B3). Each figure displays the (fast) Lomb–Scargle amplitude spectra of the injected (orange) and simulated (black) light curves for 20 mock realisations, illustrating the fidelity of the injected pulsation modes across different noise and visibility conditions. In particular, we highlight four conditions being the value of $n_{\rm CAM}$, the stellar magnitude, the stellar pollution rate (SPR; i.e. how much contaminating light that leaks into target aperture mask on average), and the mean gnomonic radial distance the target star is away from the optical axis of each camera $\vartheta_{\rm OA}$. While $n_{\rm CAM}$ and the stellar magnitude set the base noise level, the SPR and $\vartheta_{\rm OA}$ are important noise contributors. In particular, a high SPR will naturally suppress the mode amplitudes, which is evident from each panel of Fig. B1, B2, and B3 for those target stars that have a non-zero SPR. On the other hand, the higher $\vartheta_{\rm OA}$ is, the lower the instrument transmission efficiency is and, thus, the lower the mode detectability is.

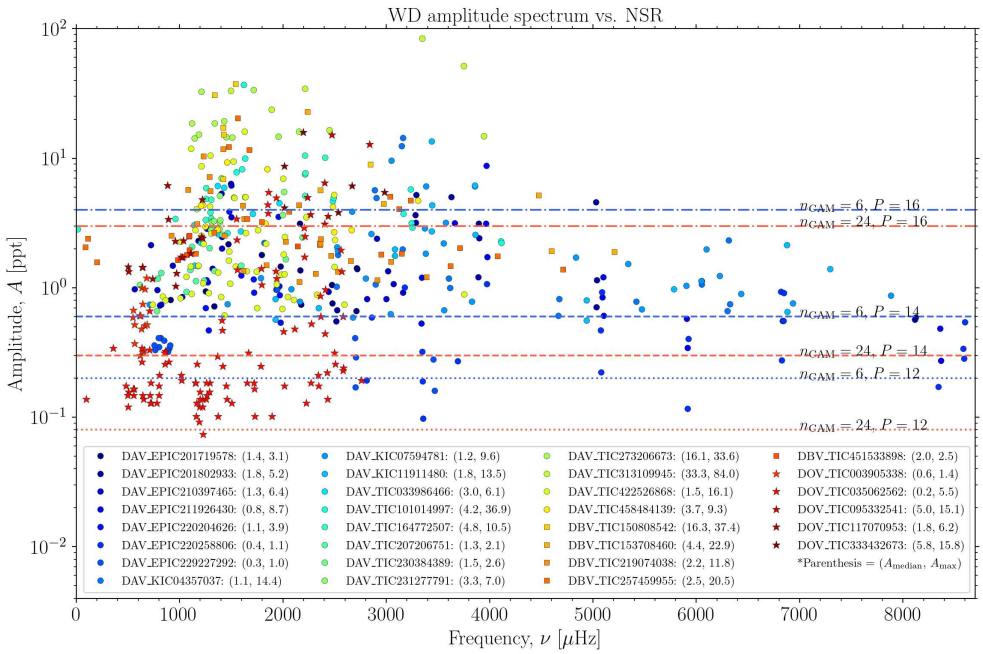


Fig. 6 Pulsation amplitude vs. NSR diagram. Each previously observed pulsator has a unique colour-coding, while DAV, DBV, and GW Vir stars are marked with circles, squares, and stars. The horizontal lines represents general time domain noise limits for $n_{\rm CAM}$ of 6 (blue) and 24 (red) as function of G-band magnitude corresponding to 12 (dotted), 14 (dashed), and 16 (dashed-dotted). Within the rounded brackets of the legend, we indicate respectively the median and maximum pulsations amplitude for each target.

Aside from the multiple noise sources that contribute to PLATO's overall noise budget, our analysis of all 30 pulsating stars simulated demonstrate that PLATO will be able to detect almost all pulsation modes in the bright end, and more than 50% of the modes for all simulations irrespective of the N-CAM visibility. The only exception are for heavily contaminated stars with SPR > 10%. Vanishing mode suppression is observed for SPR < 6% which agrees with the SPR threshold found by [97]. Based on above mentioned number statistics, the simulations presented in this work will serve as a solid benchmark for the selection of optimal WD targets for our first competitive GO proposal, while future `PlatoSim` simulations continuously will help shaping each preparatory phase before each GO call.

9 Conclusions and future prospects

PLATO's unprecedented capability to deliver two years of uninterrupted, high signal-to-noise light curves from its 26 cameras will revolutionize WD asteroseismology. By identifying common patterns in pulsation spectra of pulsating WDs, we will systematically compare observed frequencies with theoretical stellar models. This comparison will allow us to determine fundamental parameters such as WD mass through asymptotic period spacing analysis

based on model grids spanning a broad range of masses and effective temperatures. In parallel, fitting individual pulsation periods with detailed models will provide deeper insights into internal structure, effective temperature, and stratification. These models will further yield seismological distances, which can be cross-validated against *Gaia*'s precise astrometric measurements to test the reliability and robustness of asteroseismic models. Moreover, the detection of rotational splitting in non-radial pulsation modes will enable us to constrain the internal rotation periods of WDs, probing angular momentum evolution. PLATO's long-duration light curves will help uncover rare and poorly understood WD pulsator classes, such as ultra-massive WDs, ELMs, and hot DAVs, and refine our mapping of instability strips across the diverse WD spectral zoo (DAV, DBV, GW Vir).

We created a sample of 159 high-priority WD candidates ($G \leq 17$) identified in PLATO's Southern LOPS2 field using the PLATO-CS MOCKA catalogue and *Gaia* DR3, with atmospheric parameters derived via photometric modeling. This includes 118 DAs (23 ZZ Ceti candidates), 41 non-DAs (35 DBV candidates).

Simulated observations using `PlatoSim` reveal that, for pulsation periods $G \leq 12$ mag and with at least 24 co-pointing cameras ($n_{\mathrm{CAM}} = 24$), PLATO will detect nearly all relevant white dwarf pulsation modes. In contrast, with fewer cameras ($n_{\mathrm{CAM}} = 6$) and faint WDs ($G \geq 17$ mag), only a fraction of the pulsation modes are expected to be detectable due to higher noise levels. These results underscore PLATO's transformative potential to deliver a high-quality, space-based asteroseismic dataset for the white dwarf population, enabling unprecedented insights into the internal structure and evolution of stellar remnants.

Future spectroscopic and photometric observations of pulsating WDs are crucial to complement PLATO's data and enable a more thorough characterization. Ongoing and forthcoming large-scale spectroscopic surveys, such as Sloan Digital Sky Survey V [*SDSS-V*; 124] and 4MOST [125], will play a vital role in confirming spectroscopic classifications and expanding the pulsating WD sample size. In addition to the spectroscopic surveys, ongoing and upcoming photometric missions, including the TESS, alongside ground-based initiatives such as the Vera C. Rubin Observatory's Legacy Survey of Space and Time [*LSST*; 126] and *BlackGEM* [127], will provide complementary time-domain data. These combined efforts will improve our understanding of white dwarf variability, reveal new pulsation modes, and enable more precise stellar modeling. A coordinated survey of the LOPS2 region, supported by ground-based spectroscopy, will be essential to maximize the scientific return of PLATO's white dwarf program. Together, these efforts will yield a rich, well-characterized sample of pulsating white dwarfs, offering new insights into the final stages of stellar evolution.

Supplementary information.

Acknowledgements. This work presents results from the European Space Agency (ESA) space mission PLATO. The PLATO payload, the PLATO Ground Segment and PLATO data processing are joint developments of ESA and the PLATO mission consortium (PMC). Funding for the PMC is provided at national levels, in particular by countries participating in the PLATO Multilateral Agreement (Austria, Belgium, Czech Republic, Denmark, France, Germany, Italy, Netherlands, Portugal, Spain, Sweden, Switzerland, Norway, and United Kingdom) and institutions from Brazil. Members of the PLATO Consortium can be found at https://platomission.com/. The ESA PLATO mission website is https://www.cosmos.esa.int/plato. We thank the teams working for PLATO for all their work. M.U. gratefully acknowledges funding from the Research Foundation Flanders (FWO) by means of a junior postdoctoral

fellowship (grant agreement No. 1247624N). M.K. acknowledges support by the NSF under grant AST-2205736, and the NASA under grants 80NSSC22K0479, 80NSSC24K0380, and 80NSSC24K0436. P.S. acknowledges support from the Agencia Estatal de Investigación del Ministerio de Ciencia, Innovación y Universidades (MCIU/AEI) under grant "Revolucionando el conocimiento de la evolución de estrellas poco masivas" and the European Union NextGenerationEU/PRTR with reference CNS2023-143910 (DOI:10.13039/501100011033). Zs.B. acknowledges the financial support of the KKP-137523 'SeismoLab' Élvonal grant of the Hungarian Research, Development and Innovation Office (NKFIH). The research behind these results has received funding from the BELgian federal Science Policy Office (BELSPO) through PRODEX grant PLATO: ZKE2050-01-D01. We acknowledge the PLATO CS team, the simulation developers at KU Leuven, and ESA for making this mission possible.

Declarations

Conflict of interest/Competing interests The authors declare that they have no conflict of interest.
Code availability The codes used in this study are publicly available at https://ivs-kuleuven.github.io/PlatoSim3/.

Appendix A LOPS2 target list

Table A1: Parameters of DA white dwarfs modeled with pure-hydrogen atmospheres are presented, incorporating Gaia DR3 data, PLATO Input Catalog information, and photometric fit results, with targets ordered by increasing right ascension.

Name	Gaia ID	RA [deg]	Dec [deg]	Pwd	G [mag]	P [mag]	$n_{\rm CAM}$	Abundance	S. Type	$T_{\rm eff}$ [K]	$\log g$ [cm s^{-2}]	M [$M_\odot$]
WDJ033434.32-640057.11	4673757096243879168	53.64349	-64.01608	0.03	14.03	13.88	6	[He/H=0]	DA	26552^{+707}_{-707}	$7.250^{+0.029}_{-0.027}$	$0.343^{+0.011}_{-0.011}$
WDJ033823.93-575826.83	4729626958543290368	54.59983	-57.97409	0.01	16.33	16.47	6	[He/H=0]	DA	31370^{+956}_{-956}	$5.272^{+0.125}_{-0.100}$	$0.235^{+0.046}_{-0.009}$
WDJ034222.37-670935.88	4667932055438729728	55.59395	-67.15954	1.00	15.72	15.78	6	[He/H=0]	DA	15219^{+272}_{-272}	$8.258^{+0.015}_{-0.014}$	$0.771^{+0.013}_{-0.012}$
WDJ035938.19-511839.83	4828757999190736128	59.90907	-51.31099	1.00	15.76	15.89	12	[He/H=0]	DA	22359^{+300}_{-299}	$7.827^{+0.013}_{-0.012}$	$0.539^{+0.008}_{-0.009}$
WDJ040530.09-412109.11	4842194473663089920	61.37526	-41.35250	1.00	16.29	16.41	6	[He/H=0]	DA	21502^{+452}_{-451}	$7.856^{+0.018}_{-0.018}$	$0.551^{+0.013}_{-0.013}$
WDJ040532.88-505557.89	4828681514413122944	61.38920	-50.93269	0.99	15.81	15.76	12	[He/H=0]	DA	9607^{+123}_{-123}	$7.902^{+0.020}_{-0.020}$	$0.543^{+0.015}_{-0.015}$
WDJ040935.24-494219.28	4830333221396620032	62.39712	-49.70509	1.00	16.75	16.92	12	[He/H=0]	DA	31531^{+938}_{-938}	$7.833^{+0.035}_{-0.033}$	$0.565^{+0.023}_{-0.021}$
WDJ041013.13-441053.05	4838637798361005696	62.55465	-44.18141	1.00	16.64	16.82	12	[He/H=0]	DA	32618^{+593}_{-593}	$7.705^{+0.023}_{-0.022}$	$0.511^{+0.013}_{-0.012}$
WDJ041110.32-514651.04	4780544792270137088	62.79285	-51.78109	1.00	16.18	16.32	12	[He/H=0]	DA	25151^{+419}_{-419}	$7.749^{+0.019}_{-0.018}$	$0.510^{+0.012}_{-0.011}$
WDJ041114.18-370053.94	4845518095450995328	62.80898	-37.01495	1.00	16.75	16.87	6	[He/H=0]	DA	20796^{+419}_{-420}	$7.977^{+0.018}_{-0.019}$	$0.613^{+0.014}_{-0.014}$
WDJ041121.16-322614.82	4882864622796659072	62.83788	-32.43787	0.06	16.13	15.92	6	[He/H=0]	DAM	15182^{+201}_{-201}	$7.602^{+0.022}_{-0.019}$	$0.416^{+0.012}_{-0.011}$
WDJ041250.75-451012.52	4837423533408638080	63.21214	-45.16961	1.00	15.14	15.18	12	[He/H=0]	DA	13084^{+146}_{-147}	$7.931^{+0.008}_{-0.008}$	$0.569^{+0.007}_{-0.007}$
WDJ041337.30-502808.71	4782203646078747648	63.40546	-50.46942	1.00	16.37	16.47	12	[He/H=0]	DA	19330^{+286}_{-285}	$7.829^{+0.015}_{-0.015}$	$0.531^{+0.011}_{-0.010}$
WDJ041539.80-402232.69	4841120770494891520	63.91592	-40.37567	1.00	16.09	16.28	6	[He/H=0]	DA	34725^{+2317}_{-2316}	$7.428^{+0.065}_{-0.059}$	$0.421^{+0.028}_{-0.026}$
WDJ041602.97-403212.44	4841115341656167552	64.01268	-40.53702	1.00	16.11	16.22	6	[He/H=0]	DA	20144^{+408}_{-408}	$7.945^{+0.018}_{-0.017}$	$0.594^{+0.014}_{-0.013}$
WDJ041630.04-591757.19	4678664766393827328	64.12478	-59.30000	1.00	12.48	12.53	6	[He/H=0]	DA	13490^{+199}_{-198}	$7.754^{+0.014}_{-0.013}$	$0.478^{+0.010}_{-0.009}$
WDJ041711.36-545747.22	4778802753534553472	64.29762	-54.96300	0.99	15.32	15.48	6	[He/H=0]	DA	28219^{+463}_{-463}	$6.943^{+0.018}_{-0.017}$	$0.266^{+0.006}_{-0.005}$
WDJ041804.15-384519.53	4844370755067765504	64.51754	-38.75520	1.00	16.15	16.24	6	[He/H=0]	DA	18788^{+267}_{-266}	$7.902^{+0.014}_{-0.013}$	$0.567^{+0.010}_{-0.009}$
WDJ041921.96-302643.10	4884691594508544128	64.84196	-30.44520	1.00	16.58	16.67	6	[He/H=0]	DA	18122^{+250}_{-250}	$7.859^{+0.014}_{-0.013}$	$0.543^{+0.010}_{-0.009}$
WDJ041924.71-531917.10	4779427928974390272	64.85283	-53.32129	1.00	16.42	16.57	12	[He/H=0]	DA	25041^{+416}_{-415}	$7.728^{+0.019}_{-0.018}$	$0.500^{+0.012}_{-0.011}$
WDJ041930.81-352046.73	4870090943381248128	64.87816	-35.34649	1.00	16.80	16.78	6	[He/H=0]	DA	10602^{+146}_{-145}	$8.041^{+0.020}_{-0.020}$	$0.626^{+0.017}_{-0.017}$
WDJ041955.84-522122.89	4781732470986533120	64.98248	-52.35632	1.00	16.13	16.20	12	[He/H=0]	DA	15612^{+193}_{-192}	$7.861^{+0.012}_{-0.012}$	$0.538^{+0.008}_{-0.009}$
WDJ042357.67-455042.27	4789516154317811456	65.98968	-45.84736	0.99	16.67	16.41	12	[He/H=0]	DA	5562^{+32}_{-32}	$7.974^{+0.013}_{-0.013}$	$0.570^{+0.010}_{-0.011}$

Continued on next page

Name	Gaia ID	RA [deg]	Dec [deg]	Pwd	G [mag]	P [mag]	$n_{\rm CAM}$	Abundance	S. Type	$T_{\rm eff}$ [K]	$\log g$ [cm s^{-2}]	M [$M_\odot$]
WDJ043133.39-404735.67	4863952954079430272	67.88915	-40.79323	1.00	16.71	16.89	12	[He/H=0]	DA	30476^{+557}_{-557}	$7.764^{+0.023}_{-0.023}$	$0.531^{+0.014}_{-0.014}$
WDJ043254.41-325314.36	4871521270570577152	68.22689	-32.88711	0.03	16.50	16.34	6	[He/H=0]	DA	7029^{+87}_{-87}	$5.701^{+0.024}_{-0.029}$	$0.160^{+0.004}_{-0.007}$
WDJ043255.87-355729.04	4867574023826934272	68.23443	-35.95788	1.00	16.80	16.49	6	[He/H=0]	DA	4919^{+31}_{-30}	$7.843^{+0.016}_{-0.017}$	$0.488^{+0.013}_{-0.012}$
WDJ043333.60-275324.86	4891567154251463680	68.39196	-27.89027	1.00	16.59	16.30	6	[He/H=0]	DA	5083^{+15}_{-14}	$8.004^{+0.006}_{-0.006}$	$0.583^{+0.005}_{-0.005}$
WDJ043704.01-572821.62	4775127807717312640	69.26679	-57.47228	1.00	15.63	15.74	12	[He/H=0]	DA	20100^{+448}_{-448}	$8.075^{+0.018}_{-0.018}$	$0.667^{+0.015}_{-0.014}$
WDJ043859.53-285614.80	4879382984867446144	69.74802	-28.93757	1.00	16.48	16.58	6	[He/H=0]	DA	19353^{+231}_{-232}	$7.857^{+0.012}_{-0.011}$	$0.546^{+0.008}_{-0.008}$
WDJ043915.39-571900.57	4774755245074357120	69.81406	-57.31677	0.99	15.63	15.79	12	[He/H=0]	DA	29018^{+754}_{-754}	$7.119^{+0.029}_{-0.027}$	$0.312^{+0.012}_{-0.011}$
WDJ044137.51-485503.02	4785027741695161728	70.40635	-48.91746	0.01	15.22	15.40	12	[He/H=0]	DA	38956^{+1581}_{-1582}	$5.274^{+0.053}_{-nan}$	$0.200^{+0.004}_{-0.464}$
WDJ044550.77-385538.25	4818044770206932864	71.46149	-38.92727	1.00	16.76	16.96	12	[He/H=0]	DA	44971^{+5476}_{-5476}	$7.722^{+0.069}_{-0.061}$	$0.550^{+0.042}_{-0.035}$
WDJ044901.96-423414.72	4814969195665821568	72.25826	-42.57066	1.00	16.58	16.65	12	[He/H=0]	DA	15937^{+332}_{-331}	$7.922^{+0.019}_{-0.018}$	$0.571^{+0.015}_{-0.014}$
WDJ044957.96-474959.45	4786446146054306048	72.49150	-47.83327	1.00	16.04	16.14	12	[He/H=0]	DA	18533^{+225}_{-224}	$7.837^{+0.012}_{-0.012}$	$0.533^{+0.009}_{-0.008}$
WDJ045151.11-730250.29	4652838475220068992	72.96524	-73.04695	0.97	16.57	16.38	6	[He/H=0]	DA	6680^{+64}_{-64}	$7.665^{+0.019}_{-0.019}$	$0.412^{+0.013}_{-0.012}$
WDJ045312.76-442340.14	4811421896276768128	73.30335	-44.39438	1.00	15.45	15.55	12	[He/H=0]	DA	19017^{+450}_{-449}	$7.819^{+0.027}_{-0.026}$	$0.525^{+0.019}_{-0.017}$
WDJ045359.85-432247.75	4811871287295222016	73.50155	-43.37959	0.99	16.82	16.82	12	[He/H=0]	DA	11162^{+196}_{-196}	$7.606^{+0.019}_{-0.018}$	$0.404^{+0.011}_{-0.011}$
WDJ045405.87-342505.71	4873109308958466432	73.52446	-34.41821	1.00	16.13	16.15	6	[He/H=0]	DA	11960^{+153}_{-152}	$8.028^{+0.009}_{-0.010}$	$0.622^{+0.008}_{-0.008}$
WDJ045423.71-343948.35	4873054711334208256	73.59970	-34.66404	1.00	16.00	16.11	6	[He/H=0]	DA	20271^{+269}_{-269}	$7.796^{+0.011}_{-0.011}$	$0.518^{+0.007}_{-0.008}$
WDJ045440.28-342651.96	4873061617641604864	73.66829	-34.44714	1.00	15.98	16.08	6	[He/H=0]	DA	19414^{+287}_{-287}	$7.802^{+0.013}_{-0.012}$	$0.519^{+0.008}_{-0.009}$
WDJ045514.63-544145.41	4776747972460494208	73.80995	-54.69619	1.00	14.37	14.45	12	[He/H=0]	DA	16659^{+215}_{-215}	$7.797^{+0.011}_{-0.011}$	$0.508^{+0.008}_{-0.008}$
WDJ045527.27-625844.61	4665237908354588288	73.86402	-62.97854	1.00	14.97	14.97	6	[He/H=0]	DAV	11106^{+115}_{-115}	$7.840^{+0.012}_{-0.011}$	$0.514^{+0.009}_{-0.008}$
WDJ045535.94-292859.95	4876689387538123008	73.89973	-29.48293	1.00	15.01	15.07	6	[He/H=0]	DA	16230^{+133}_{-134}	$7.218^{+0.007}_{-0.007}$	$0.296^{+0.003}_{-0.002}$
WDJ045551.33-705541.81	4654695103690489856	73.96579	-70.92856	0.99	16.49	16.45	6	[He/H=0]	DA	10324^{+238}_{-237}	$7.934^{+0.032}_{-0.030}$	$0.563^{+0.026}_{-0.024}$
WDJ045648.37-435123.35	4811658909752355584	74.20160	-43.85660	1.00	16.12	16.22	12	[He/H=0]	DA	19649^{+299}_{-298}	$7.864^{+0.014}_{-0.014}$	$0.550^{+0.010}_{-0.010}$
WDJ045658.40-531026.40	4782942513595999872	74.24372	-53.17393	1.00	16.79	16.90	12	[He/H=0]	DA	21331^{+443}_{-443}	$7.483^{+0.022}_{-0.021}$	$0.393^{+0.011}_{-0.009}$
WDJ045713.32-280752.72	4880286371109059712	74.30576	-28.13126	0.99	13.93	14.13	6	[He/H=0]	DA	39575^{+335}_{-335}	$7.377^{+0.029}_{-0.034}$	$0.419^{+0.013}_{-0.014}$
WDJ045732.31-641010.95	4664651250184794368	74.38533	-64.16834	0.99	16.95	16.80	6	[He/H=0]	DA	6293^{+103}_{-104}	$7.340^{+0.055}_{-0.050}$	$0.282^{+0.027}_{-0.022}$
WDJ050042.52-301637.70	4876440794831381760	75.17721	-30.27707	0.98	16.63	16.84	6	[He/H=0]	DA	97759^{+7538}_{-7538}	$7.587^{+0.083}_{-0.071}$	$0.645^{+0.033}_{-0.030}$
WDJ050323.06-570122.22	4763928766392708864	75.84610	-57.02269	0.99	16.11	16.30	12	[He/H=0]	DA	41388^{+3381}_{-3381}	$7.393^{+0.051}_{-0.047}$	$0.430^{+0.025}_{-0.025}$
WDJ050458.06-494143.53	4785276918518079616	76.24243	-49.69469	1.00	15.90	15.96	12	[He/H=0]	DA	15133^{+202}_{-202}	$7.888^{+0.013}_{-0.012}$	$0.551^{+0.010}_{-0.009}$

Continued on next page

Name	Gaia ID	RA [deg]	Dec [deg]	Pwd	G [mag]	P [mag]	$n_{\rm CAM}$	Abundance	S. Type	$T_{\rm eff}$ [K]	$\log g$ [cm s^{-2}]	M [$M_\odot$]
WDJ051223.04-414526.04	4812859061053900928	78.09605	-41.75724	1.00	16.84	17.03	18	[He/H=0]	DA	45626^{+5163}_{-5162}	$7.836^{+0.062}_{-0.056}$	$0.600^{+0.041}_{-0.036}$
WDJ051327.80-412751.88	4812870056170125568	78.36593	-41.46307	1.00	15.98	15.95	18	[He/H=0]	DA	10122^{+162}_{-161}	$7.957^{+0.022}_{-0.022}$	$0.575^{+0.019}_{-0.017}$
WDJ051537.22-322454.03	4827311522925744768	78.90534	-32.41507	1.00	16.32	16.41	12	[He/H=0]	DA	18110^{+301}_{-301}	$7.653^{+0.015}_{-0.015}$	$0.446^{+0.010}_{-0.008}$
WDJ052042.54-361610.81	4822236743909344256	80.17721	-36.26987	1.00	16.39	16.49	12	[He/H=0]	DA	18504^{+304}_{-303}	$7.853^{+0.015}_{-0.015}$	$0.541^{+0.011}_{-0.010}$
WDJ052422.51-514054.85	4772418885944906112	81.09419	-51.68156	1.00	15.92	15.96	24	[He/H=0]	DA	13328^{+190}_{-190}	$7.938^{+0.012}_{-0.012}$	$0.574^{+0.009}_{-0.010}$
WDJ052446.21-381837.14	4819672528450697984	81.19251	-38.31044	0.99	16.60	16.61	18	[He/H=0]	DA	20887^{+604}_{-604}	$7.785^{+0.028}_{-0.027}$	$0.514^{+0.019}_{-0.017}$
WDJ052448.16-464100.34	4798944672685041152	81.20107	-46.68432	0.99	16.18	16.09	24	[He/H=0]	DA	8578^{+92}_{-92}	$7.873^{+0.017}_{-0.017}$	$0.524^{+0.013}_{-0.013}$
WDJ052518.96-302018.13	2905372374461903488	81.32921	-30.33830	0.98	16.76	16.77	12	[He/H=0]	DA	11616^{+109}_{-109}	$7.904^{+0.010}_{-0.010}$	$0.550^{+0.008}_{-0.008}$
WDJ052528.17-385410.97	4807583638623283584	81.36772	-38.90262	0.04	16.23	16.04	18	[He/H=0]	DAM	16654^{+326}_{-325}	$7.319^{+0.081}_{-0.097}$	$0.325^{+0.033}_{-0.035}$
WDJ052545.71-544407.34	4769992263782028544	81.44031	-54.73556	1.00	16.47	16.61	18	[He/H=0]	DA	26078^{+465}_{-464}	$7.674^{+0.020}_{-0.021}$	$0.480^{+0.012}_{-0.011}$
WDJ052548.76-671611.58	4658691072554066560	81.45281	-67.27038	1.00	16.91	16.86	6	[He/H=0]	DA	10493^{+328}_{-328}	$8.127^{+0.047}_{-0.043}$	$0.679^{+0.041}_{-0.038}$
WDJ052639.42-353557.43	4822043831436262784	81.66460	-35.59954	0.97	16.17	16.12	12	[He/H=0]	DA	9522^{+78}_{-78}	$7.304^{+0.015}_{-0.015}$	$0.288^{+0.006}_{-0.007}$
WDJ052724.33-310655.56	2905067333001582720	81.85065	-31.11690	1.00	15.96	15.99	12	[He/H=0]	DA	13539^{+238}_{-237}	$8.853^{+0.010}_{-0.010}$	$1.130^{+0.006}_{-0.006}$
WDJ052844.01-430449.21	4805691447831511680	82.18385	-43.08050	0.99	16.09	16.04	12	[He/H=0]	DA	10149^{+124}_{-123}	$8.627^{+0.015}_{-0.015}$	$1.000^{+0.012}_{-0.012}$
WDJ052912.10-430334.49	4805782462481529600	82.30017	-43.05951	1.00	16.17	16.19	12	[He/H=0]	DA	11669^{+180}_{-180}	$7.715^{+0.014}_{-0.013}$	$0.454^{+0.009}_{-0.009}$
WDJ053100.49-455801.14	4799224635833122304	82.75279	-45.96644	1.00	16.66	16.63	24	[He/H=0]	DA	10387^{+184}_{-184}	$7.948^{+0.025}_{-0.025}$	$0.571^{+0.021}_{-0.020}$
WDJ053203.91-653609.91	4660769493122896128	83.01610	-65.60277	1.00	16.89	16.89	12	[He/H=0]	DA	11330^{+250}_{-250}	$7.904^{+0.025}_{-0.025}$	$0.549^{+0.020}_{-0.019}$
WDJ053306.78-560353.38	4766810380210581632	83.27841	-56.06476	1.00	15.93	15.92	18	[He/H=0]	DA	10915^{+121}_{-121}	$8.345^{+0.014}_{-0.013}$	$0.820^{+0.012}_{-0.011}$
WDJ053343.43-271350.08	2908425653829891712	83.43077	-27.23082	1.00	15.61	15.73	12	[He/H=0]	DA	22113^{+235}_{-235}	$9.004^{+0.007}_{-0.007}$	$1.204^{+0.004}_{-0.003}$
WDJ053640.24-325454.63	2901629916055849472	84.16764	-32.91517	1.00	16.82	16.92	12	[He/H=0]	DA	19138^{+509}_{-509}	$7.843^{+0.023}_{-0.022}$	$0.538^{+0.016}_{-0.015}$
WDJ053753.46-475805.10	4795556287084999552	84.47255	-47.96814	1.00	15.59	15.71	24	[He/H=0]	DA	21643^{+390}_{-391}	$8.049^{+0.016}_{-0.015}$	$0.656^{+0.012}_{-0.012}$
WDJ053939.69-664157.85	4659528969150132096	84.91658	-66.69852	1.00	15.98	15.99	12	[He/H=0]	DA	11868^{+263}_{-264}	$7.912^{+0.021}_{-0.021}$	$0.555^{+0.017}_{-0.016}$
WDJ054412.15-352547.00	2888817253850677760	86.05097	-35.43001	1.00	15.23	15.25	12	[He/H=0]	DA	12573^{+186}_{-185}	$7.888^{+0.010}_{-0.010}$	$0.544^{+0.008}_{-0.008}$
WDJ054458.33-401940.13	4805139866655106944	86.24291	-40.32770	1.00	16.96	16.95	24	[He/H=0]	DA	11596^{+268}_{-269}	$7.942^{+0.025}_{-0.024}$	$0.571^{+0.020}_{-0.019}$
WDJ055428.05-402555.11	4804209684114310784	88.61677	-40.43208	1.00	16.63	16.65	24	[He/H=0]	DA	12570^{+338}_{-337}	$8.354^{+0.021}_{-0.020}$	$0.829^{+0.018}_{-0.018}$
WDJ055814.63-373426.02	2884285498084601600	89.56110	-37.57417	0.99	14.32	14.53	24	[He/H=0]	DA	54126^{+4471}_{-4471}	$7.309^{+0.041}_{-0.038}$	$0.434^{+0.025}_{-0.021}$
WDJ060013.07-545516.04	5500308124837433984	90.05431	-54.92130	1.00	16.21	16.21	18	[He/H=0]	DA	10785^{+139}_{-139}	$8.202^{+0.016}_{-0.016}$	$0.727^{+0.014}_{-0.014}$
WDJ060502.73-481958.44	5554202096021588992	91.26148	-48.33261	1.00	15.83	16.00	24	[He/H=0]	DA	31780^{+705}_{-705}	$7.702^{+0.023}_{-0.022}$	$0.508^{+0.013}_{-0.013}$

Continued on next page

Name	Gaia ID	RA [deg]	Dec [deg]	Pwd	G [mag]	P [mag]	n_{CAM}	Abundance	S. Type	T_{eff} [K]	$\log g$ [cm s^{-2}]	M [$M_{\odot}$]
WDJ060843.80-530134.27	5548648634588556288	92.18144	-53.02523	0.99	15.96	15.90	24	[He/H=0]	DA	9560^{+98}_{-98}	$7.887^{+0.017}_{-0.016}$	$0.535^{+0.012}_{-0.013}$
WDJ061958.87-414337.84	5571715735704543360	94.99655	-41.72883	1.00	15.41	15.35	24	[He/H=0]	DA	9450^{+86}_{-86}	$7.933^{+0.015}_{-0.014}$	$0.560^{+0.012}_{-0.011}$
WDJ062312.62-374128.04	5575007845317435648	95.80295	-37.69113	0.98	12.02	12.23	24	[He/H=0]	DA	50596^{+4372}_{-4371}	$7.120^{+0.045}_{-0.042}$	$0.375^{+0.024}_{-0.020}$
WDJ062425.79-325727.38	2892228919840595072	96.10746	-32.95841	0.99	15.42	15.40	12	[He/H=0]	DAB	13614^{+142}_{-141}	$7.733^{+0.010}_{-0.009}$	$0.469^{+0.006}_{-0.006}$
WDJ064428.73-283238.07	2918665577420228480	101.11914	-28.54434	0.99	16.42	16.34	12	[He/H=0]	DA	8873^{+54}_{-54}	$7.839^{+0.011}_{-0.010}$	$0.507^{+0.008}_{-0.008}$
WDJ064802.46-483039.16	5551402808137892864	102.01025	-48.51111	1.00	16.73	16.74	24	[He/H=0]	DA	11551^{+201}_{-201}	$7.920^{+0.019}_{-0.019}$	$0.559^{+0.015}_{-0.015}$
WDJ064856.09-252346.96	2921786919133198848	102.23357	-25.39623	1.00	13.63	13.78	6	[He/H=0]	DA	27028^{+213}_{-213}	$7.869^{+0.008}_{-0.008}$	$0.571^{+0.006}_{-0.005}$
WDJ065330.21-395429.12	5564029702750970112	103.37551	-39.90710	0.99	15.92	15.70	24	[He/H=0]	DA	6177^{+27}_{-27}	$8.046^{+0.009}_{-0.010}$	$0.617^{+0.008}_{-0.009}$
WDJ065335.34-395533.29	5564028981196462336	103.39689	-39.92490	0.99	15.35	15.19	24	[He/H=0]	DA	6975^{+38}_{-39}	$7.965^{+0.011}_{-0.011}$	$0.571^{+0.009}_{-0.009}$
WDJ065355.03-562447.16	5484935887129131648	103.47934	-56.41298	1.00	16.62	16.79	24	[He/H=0]	DA	30025^{+701}_{-701}	$8.719^{+0.022}_{-0.021}$	$1.071^{+0.014}_{-0.015}$
WDJ065705.91-390935.68	5564171814627287296	104.27292	-39.16058	0.99	14.98	14.77	6	[He/H=0]	DA	6356^{+26}_{-26}	$8.068^{+0.009}_{-0.009}$	$0.631^{+0.008}_{-0.008}$
WDJ070219.72-585009.02	5480556532316697216	105.58175	-58.83494	1.00	14.58	14.61	12	[He/H=0]	DA	12929^{+179}_{-180}	$8.435^{+0.009}_{-0.009}$	$0.882^{+0.007}_{-0.007}$
WDJ070520.53-204642.21	2929364817693200640	106.33599	-20.77873	1.00	16.50	16.67	6	[He/H=0]	DAH	29476^{+402}_{-402}	$8.880^{+0.012}_{-0.013}$	$1.153^{+0.007}_{-0.007}$
WDJ070925.08-320507.33	5604216131195297664	107.35349	-32.08313	1.00	15.60	15.55	6	[He/H=0]	DA	9736^{+149}_{-149}	$7.915^{+0.023}_{-0.023}$	$0.550^{+0.019}_{-0.017}$
WDJ071039.41-414424.56	5561160355360035456	107.66520	-41.74069	1.00	15.79	15.77	24	[He/H=0]	DAH	10074^{+91}_{-90}	$7.933^{+0.014}_{-0.013}$	$0.562^{+0.011}_{-0.011}$
WDJ071051.17-342107.14	5602672550010235008	107.71328	-34.35244	1.00	16.24	16.22	12	[He/H=0]	DA	10707^{+127}_{-126}	$7.968^{+0.014}_{-0.013}$	$0.584^{+0.011}_{-0.011}$
WDJ071114.41-251815.05	5617205933369326592	107.80948	-25.30330	0.99	14.45	14.42	6	[He/H=0]	DA	10677^{+39}_{-40}	$7.141^{+0.004}_{-0.004}$	$0.251^{+0.001}_{-0.001}$
WDJ071516.58-702505.62	5267418883330985856	108.81764	-70.41772	1.00	14.01	14.20	12	[He/H=0]	DA	37834^{+1551}_{-1552}	$7.737^{+0.026}_{-0.025}$	$0.538^{+0.016}_{-0.014}$
WDJ071550.55-370642.20	5589354543620145024	108.95916	-37.11102	1.00	16.59	16.43	12	[He/H=0]	DA	7195^{+59}_{-60}	$8.399^{+0.013}_{-0.014}$	$0.849^{+0.012}_{-0.012}$
WDJ071751.88-282928.84	5606764386835758720	109.46577	-28.49113	1.00	16.42	16.39	6	[He/H=0]	DA	10444^{+50}_{-50}	$7.988^{+0.008}_{-0.007}$	$0.595^{+0.006}_{-0.007}$
WDJ072047.91-314702.73	5604890028746727552	110.19944	-31.78405	0.06	14.57	14.45	6	[He/H=0]	DA	28292^{+654}_{-654}	$6.918^{+0.027}_{-0.026}$	$0.261^{+0.008}_{-0.008}$
WDJ072320.10-274721.58	5612710511362093184	110.83391	-27.78942	1.00	14.52	14.69	6	[He/H=0]	DA	33637^{+699}_{-699}	$7.765^{+0.017}_{-0.018}$	$0.539^{+0.011}_{-0.010}$
WDJ072717.48-332838.16	5592485716514387584	111.82298	-33.47756	1.00	16.55	16.55	12	[He/H=0]	DA	11775^{+297}_{-298}	$7.714^{+0.023}_{-0.022}$	$0.454^{+0.016}_{-0.015}$
WDJ073326.40-445325.34	5510964144860346496	113.36057	-44.89046	0.99	15.34	15.26	12	[He/H=0]	DA	9181^{+82}_{-82}	$7.937^{+0.014}_{-0.015}$	$0.561^{+0.012}_{-0.011}$
WDJ073337.81-425357.25	5536077746353130240	113.40796	-42.89623	1.00	14.19	14.24	12	[He/H=0]	DA	14726^{+223}_{-223}	$8.111^{+0.014}_{-0.014}$	$0.678^{+0.012}_{-0.012}$
WDJ073338.28-281623.17	5611744006283630720	113.40918	-28.27263	1.00	15.96	15.97	6	[He/H=0]	DA	12351^{+62}_{-62}	$8.373^{+0.004}_{-0.005}$	$0.841^{+0.004}_{-0.004}$
WDJ074152.84-570844.74	5295512298775133824	115.46997	-57.14541	1.00	15.15	15.25	12	[He/H=0]	DA	19549^{+311}_{-311}	$7.668^{+0.014}_{-0.014}$	$0.458^{+0.008}_{-0.008}$
WDJ074613.81-302550.93	5598661329740179712	116.55786	-30.43134	1.00	16.03	16.01	6	[He/H=0]	DA	10754^{+172}_{-172}	$7.923^{+0.018}_{-0.018}$	$0.558^{+0.014}_{-0.014}$

Continued on next page

Name	Gaia ID	RA [deg]	Dec [deg]	Pwd	G [mag]	P [mag]	$n_{\rm CAM}$	Abundance	S. Type	$T_{\rm eff}$ [K]	$\log g$ [cm s^{-2}]	M [$M_\odot$]
WDJ075308.14-674731.38	5273943488410008832	118.30118	-67.79867	1.00	13.78	13.53	12	[He/H=0]	DA	5636^{+12}_{-12}	$7.969^{+0.006}_{-0.005}$	$0.567^{+0.005}_{-0.004}$
WDJ075328.47-511436.98	5513896164414899456	118.36809	-51.24283	0.99	15.61	15.53	12	[He/H=0]	DAH	9117^{+81}_{-81}	$8.343^{+0.013}_{-0.013}$	$0.815^{+0.012}_{-0.011}$
WDJ075643.91-545348.89	5296195267296378112	119.18267	-54.89675	1.00	15.52	15.57	12	[He/H=0]	DA	11549^{+445}_{-445}	$7.871^{+0.046}_{-0.044}$	$0.532^{+0.036}_{-0.032}$
WDJ080200.19-532750.82	5512466799294681472	120.50156	-53.46395	0.08	15.82	15.64	6	[He/H=0]	DA	16937^{+311}_{-311}	$7.573^{+0.019}_{-0.019}$	$0.410^{+0.011}_{-0.010}$
WDJ081227.07-352943.32	5544743925212648320	123.11242	-35.49550	1.00	14.35	14.14	12	[He/H=0]	DAH	6238^{+24}_{-24}	$8.179^{+0.008}_{-0.008}$	$0.701^{+0.008}_{-0.007}$
WDJ082126.70-670320.02	5272690766709543680	125.35673	-67.05263	1.00	15.08	14.76	6	[He/H=0]	DA	4807^{+39}_{-40}	$7.937^{+0.020}_{-0.020}$	$0.541^{+0.017}_{-0.016}$
WDJ083151.91-534032.52	5321056462156468480	127.96650	-53.67625	1.00	14.45	14.62	6	[He/H=0]	DA	28395^{+532}_{-532}	$7.810^{+0.020}_{-0.018}$	$0.546^{+0.013}_{-0.012}$
WDJ083246.58-574125.49	5315128548292806656	128.19400	-57.69018	1.00	16.69	16.69	6	[He/H=0]	DA	11812^{+222}_{-223}	$8.039^{+0.019}_{-0.019}$	$0.628^{+0.016}_{-0.016}$
WDJ083759.16-501745.76	5322090003089341440	129.49465	-50.29528	1.00	14.60	14.61	6	[He/H=0]	DA	12163^{+194}_{-194}	$8.259^{+0.013}_{-0.013}$	$0.767^{+0.011}_{-0.012}$
WDJ084215.26-555628.51	5316824544982104960	130.56328	-55.94139	1.00	16.52	16.49	6	[He/H=0]	DA	10358^{+181}_{-182}	$7.933^{+0.026}_{-0.025}$	$0.563^{+0.020}_{-0.020}$
WDJ085102.69-615517.65	5298297567892486656	132.76058	-61.92144	1.00	14.71	14.82	6	[He/H=0]	DA	19665^{+266}_{-266}	$7.961^{+0.012}_{-0.012}$	$0.601^{+0.010}_{-0.009}$

Table A2: Parameters of white dwarfs modeled with mixed H/He atmospheres are presented, incorporating Gaia DR3 data, PLATO Input Catalog information, and values derived from our photometric fits, with targets ordered by increasing right ascension.

Name	Gaia ID	RA [deg]	Dec [deg]	Pwd	G [mag]	P [mag]	n_{CAM}	Abundance	S. Type	T_{eff} [K]	$\log g$ [cm s^{-2}]	M [$M_{\odot}$]
WDJ033117.34-592537.38	4729070979320996096	52.82229	-59.42707	1.00	16.25	16.42	6	[log H/He=-5.00]	DB	39107^{+1019}_{-1020}	$7.801^{+0.026}_{-0.024}$	$0.535^{+0.015}_{-0.015}$
WDJ041909.91-535045.31	4779379172505736832	64.79099	-53.84642	1.00	15.27	15.36	12	[log H/He=-5.00]	DB	17617^{+496}_{-497}	$7.871^{+0.028}_{-0.027}$	$0.524^{+0.021}_{-0.020}$
WDJ042211.36-474142.02	4788896304637763072	65.54690	-47.69497	1.00	15.23	15.34	12	[log H/He=-5.00]	DB	19960^{+515}_{-515}	$7.830^{+0.020}_{-0.019}$	$0.508^{+0.014}_{-0.013}$
WDJ042432.05-545539.23	4778990563864168448	66.13233	-54.92781	1.00	16.91	16.95	12	[log H/He=-5.00]	DB	12985^{+267}_{-267}	$7.876^{+0.028}_{-0.026}$	$0.517^{+0.022}_{-0.019}$
WDJ050007.86-600728.79	4761685522153733760	75.03280	-60.12458	1.00	16.29	16.34	12	[log H/He=-5.00]	DB	14181^{+277}_{-277}	$7.901^{+0.023}_{-0.023}$	$0.533^{+0.017}_{-0.017}$
WDJ061614.26-591227.41	5482551252566796928	94.05898	-59.20900	1.00	13.95	14.02	24	[log H/He=-5.00]	DB	14336^{+303}_{-303}	$7.859^{+0.027}_{-0.025}$	$0.511^{+0.020}_{-0.018}$
WDJ044427.35-351745.09	4867104257483687040	71.11383	-35.29618	1.00	15.68	15.71	6	[log H/He=-5.00]	DBA	12793^{+179}_{-180}	$8.125^{+0.017}_{-0.017}$	$0.662^{+0.015}_{-0.015}$
WDJ045153.75-254914.73	4881672923991046400	72.97381	-25.82079	1.00	16.43	16.41	6	[log H/He=-5.00]	DBAZ	10237^{+28}_{-28}	$8.038^{+0.005}_{-0.006}$	$0.604^{+0.004}_{-0.005}$
WDJ052330.80-472219.55	4797409582653745152	80.87843	-47.37214	1.00	16.69	16.80	24	[log H/He=-5.00]	DBV	19045^{+766}_{-765}	$7.858^{+0.037}_{-0.034}$	$0.520^{+0.027}_{-0.024}$
WDJ041724.58-673236.77	4668242152077665024	64.35251	-67.54344	1.00	16.63	16.75	6	[log H/He=-5.00]	DB	17419^{+875}_{-874}	$7.671^{+0.053}_{-0.049}$	$0.428^{+0.034}_{-0.029}$
WDJ042610.85-465847.47	4789144175789941888	66.54522	-46.98000	1.00	16.78	16.91	12	[log H/He=-5.00]	DB	20442^{+819}_{-819}	$7.831^{+0.028}_{-0.027}$	$0.510^{+0.019}_{-0.019}$
WDJ043151.06-532929.85	4780712394777586560	67.96298	-53.49164	1.00	16.98	17.13	12	[log H/He=-5.00]	DB	28181^{+1218}_{-1217}	$7.806^{+0.035}_{-0.032}$	$0.514^{+0.023}_{-0.020}$
WDJ050510.82-613924.40	4760710942535282560	76.29501	-61.65674	1.00	16.91	17.03	6	[log H/He=-5.00]	DB	21235^{+713}_{-714}	$8.181^{+0.023}_{-0.022}$	$0.709^{+0.019}_{-0.020}$
WDJ053423.94-381444.86	4808986478021189120	83.59984	-38.24568	1.00	16.91	17.05	12	[log H/He=-5.00]	DB	26509^{+1437}_{-1437}	$7.536^{+0.038}_{-0.036}$	$0.401^{+0.019}_{-0.017}$
WDJ054007.06-651807.95	4660085867450146560	85.02894	-65.30190	1.00	16.50	16.60	12	[log H/He=-5.00]	DB	17084^{+1291}_{-1291}	$7.739^{+0.091}_{-0.078}$	$0.458^{+0.062}_{-0.048}$
WDJ054657.41-305153.89	2903068214703934848	86.73922	-30.86496	1.00	16.51	16.64	12	[log H/He=-5.00]	DB	25266^{+1650}_{-1649}	$8.226^{+0.019}_{-0.018}$	$0.742^{+0.017}_{-0.015}$
WDJ055635.50-561006.57	4767225652008399104	89.14807	-56.16833	1.00	15.44	15.56	24	[log H/He=-5.00]	DB	19561^{+489}_{-489}	$8.232^{+0.020}_{-0.019}$	$0.739^{+0.017}_{-0.017}$
WDJ060612.38-723414.20	5266145236552677632	91.55152	-72.57079	1.00	16.67	16.77	6	[log H/He=-5.00]	DB	18259^{+742}_{-742}	$7.453^{+0.038}_{-0.035}$	$0.348^{+0.018}_{-0.015}$
WDJ060740.96-285302.51	2897810350100517504	91.92038	-28.88393	1.00	16.27	16.39	12	[log H/He=-5.00]	DB	18283^{+264}_{-265}	$7.789^{+0.014}_{-0.013}$	$0.484^{+0.010}_{-0.009}$
WDJ061109.12-703921.89	5278615205944625664	92.78797	-70.65557	1.00	16.87	16.99	6	[log H/He=-5.00]	DB	26597^{+1411}_{-1411}	$7.760^{+0.042}_{-0.039}$	$0.490^{+0.027}_{-0.024}$
WDJ061238.45-325357.56	2892795821161588736	93.16004	-32.89928	1.00	16.23	16.34	12	[log H/He=-5.00]	DB	19180^{+484}_{-484}	$7.657^{+0.022}_{-0.021}$	$0.427^{+0.013}_{-0.013}$
WDJ061524.39-384823.63	5574654180530308736	93.85156	-38.80646	1.00	16.55	16.68	24	[log H/He=-5.00]	DB	25422^{+827}_{-826}	$7.768^{+0.020}_{-0.019}$	$0.491^{+0.012}_{-0.013}$
WDJ061856.82-372607.54	5575200775248718976	94.73673	-37.43540	1.00	16.45	16.58	24	[log H/He=-5.00]	DB	22594^{+1746}_{-1746}	$7.787^{+0.022}_{-0.020}$	$0.493^{+0.015}_{-0.014}$

Continued on next page

Name	Gaia ID	RA [deg]	Dec [deg]	Pwd	G [mag]	P [mag]	$n_{\rm CAM}$	Abundance	S. Type	$T_{\rm eff}$ [K]	$\log g$ [cm s^{-2}]	M [$M_\odot$]
WDJ062000.90-233500.19	2936643760765256576	95.00382	-23.58340	1.00	16.64	16.71	6	[log H/He=-5.00]	DB	21047^{+603}_{-604}	$7.682^{+0.022}_{-0.022}$	$0.442^{+0.014}_{-0.013}$
WDJ063814.10-694335.39	5278903110486861312	99.55865	-69.72632	1.00	16.79	16.95	12	[log H/He=-5.00]	DB	32439^{+1115}_{-1115}	$8.047^{+0.029}_{-0.028}$	$0.646^{+0.023}_{-0.021}$
WDJ063845.14-470141.00	5552665081846145024	99.68799	-47.02795	1.00	16.76	16.86	24	[log H/He=-5.00]	DB	17512^{+775}_{-775}	$7.792^{+0.048}_{-0.044}$	$0.484^{+0.033}_{-0.030}$
WDJ064648.90-525349.76	5498647381243346176	101.70365	-52.89709	1.00	15.91	16.03	24	[log H/He=-5.00]	DB	18988^{+633}_{-633}	$7.930^{+0.030}_{-0.028}$	$0.558^{+0.023}_{-0.021}$
WDJ064747.51-270813.49	2919284671187233280	101.94803	-27.13727	1.00	16.79	16.92	6	[log H/He=-5.00]	DB	28620^{+581}_{-582}	$7.893^{+0.018}_{-0.019}$	$0.557^{+0.013}_{-0.013}$
WDJ065112.06-440937.57	5562002134589548032	102.80011	-44.16025	1.00	16.62	16.74	24	[log H/He=-5.00]	DB	18778^{+899}_{-899}	$7.625^{+0.044}_{-0.040}$	$0.413^{+0.026}_{-0.023}$
WDJ065703.65-433414.37	5559127976835354624	104.26542	-43.57085	1.00	16.41	16.54	24	[log H/He=-5.00]	DB	18403^{+841}_{-841}	$7.760^{+0.045}_{-0.041}$	$0.471^{+0.030}_{-0.027}$
WDJ065957.09-291701.35	5608058473357824128	104.98775	-29.28362	0.91	16.09	16.04	6	[log H/He=-5.00]	DB	21363^{+1236}_{-1237}	$7.574^{+0.022}_{-0.022}$	$0.400^{+0.012}_{-0.012}$
WDJ070918.12-302728.87	5604654870693369984	107.32535	-30.45811	1.00	16.33	16.48	6	[log H/He=-5.00]	DB	29970^{+642}_{-643}	$7.723^{+0.017}_{-0.016}$	$0.481^{+0.011}_{-0.009}$
WDJ073920.28-262915.39	5613838438495596032	114.83438	-26.48768	1.00	16.25	16.37	6	[log H/He=-5.00]	DB	19624^{+303}_{-303}	$7.876^{+0.015}_{-0.014}$	$0.530^{+0.011}_{-0.010}$
WDJ074250.12-544920.12	5488182813687216000	115.70893	-54.82214	1.00	16.90	16.99	18	[log H/He=-5.00]	DB	19127^{+1003}_{-1002}	$8.005^{+0.047}_{-0.044}$	$0.600^{+0.038}_{-0.034}$
WDJ074521.91-432803.38	5532479697634251776	116.34119	-43.46757	1.00	16.75	16.86	12	[log H/He=-5.00]	DB	19536^{+736}_{-735}	$8.289^{+0.031}_{-0.030}$	$0.775^{+0.027}_{-0.026}$
WDJ081612.57-402513.53	5539643909237818880	124.05225	-40.42045	1.00	16.08	16.21	12	[log H/He=-5.00]	DB	21792^{+1440}_{-1441}	$7.785^{+0.025}_{-0.024}$	$0.490^{+0.018}_{-0.016}$
WDJ081827.11-460309.83	5519761028164909568	124.61303	-46.05263	1.00	16.97	17.06	12	[log H/He=-5.00]	DB	17228^{+988}_{-987}	$7.843^{+0.062}_{-0.057}$	$0.508^{+0.046}_{-0.039}$
WDJ082109.21-500114.40	5514870018179554560	125.28835	-50.02063	0.99	16.47	16.62	12	[log H/He=-5.00]	DB	31577^{+977}_{-978}	$7.314^{+0.030}_{-0.031}$	$0.343^{+0.014}_{-0.015}$
WDJ083341.91-655530.74	5272852979034659072	128.42466	-65.92519	1.00	16.71	16.83	6	[log H/He=-5.00]	DB	19752^{+597}_{-596}	$7.908^{+0.025}_{-0.024}$	$0.547^{+0.019}_{-0.017}$
WDJ083942.55-535949.14	5317871245692348032	129.92690	-53.99688	1.00	16.99	17.10	6	[log H/He=-5.00]	DB	20988^{+1040}_{-1039}	$7.882^{+0.032}_{-0.032}$	$0.536^{+0.024}_{-0.022}$
WDJ085424.48-491724.58	5328333889104483712	133.60189	-49.29007	1.00	15.77	15.92	6	[log H/He=-5.00]	DB	30045^{+977}_{-977}	$7.901^{+0.025}_{-0.024}$	$0.564^{+0.018}_{-0.017}$

Appendix B Amplitude spectra from `PlatoSim`

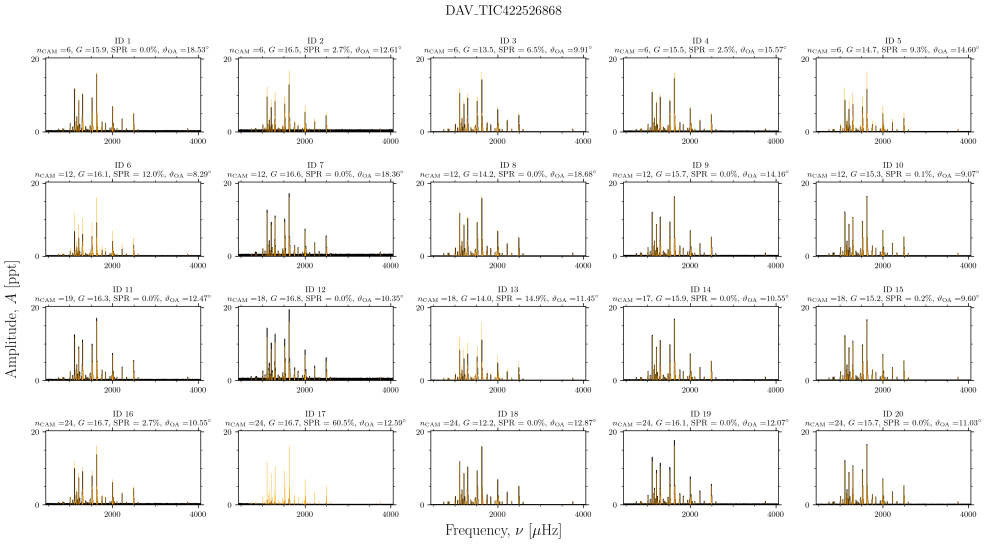


Fig. B1 Amplitude spectra of the DAV star TIC 422526868 (G29-38). Each subplot represents one of the 20 mock WD stars (with increasing ID from upper-left to lower-right panel), and shows the (fast) Lomb-Scargle amplitude spectrum of the simulated (black lines) and injected (orange lines) light curve. The title caption above each panel details information about the mock WD star simulated.

References

[1] Fontaine, G., Brassard, P., Bergeron, P.: The Potential of White Dwarf Cosmochronology. PASP **113**(782), 409–435 (2001) https://doi.org/10.1086/319535

[2] Woosley, S.E., Heger, A.: The Remarkable Deaths of 9-11 Solar Mass Stars. ApJ **810**, 34 (2015) https://doi.org/10.1088/0004-637X/810/1/34 arXiv:1505.06712 [astro-ph.SR]

[3] Althaus, L.G., Córsico, A.H., Isern, J., García-Berro, E.: Evolutionary and pulsational properties of white dwarf stars. A&A Rev. **18**(4), 471–566 (2010) https://doi.org/10.1007/s00159-010-0033-1 arXiv:1007.2659 [astro-ph.SR]

[4] Saumon, D., Blouin, S., Tremblay, P.-E.: Current challenges in the physics of white dwarf stars. Phys. Rep. **988**, 1–63 (2022) https://doi.org/10.1016/j.physrep.2022.09.001 arXiv:2209.02846 [astro-ph.SR]

[5] Guidry, J.A., Vanderbosch, Z.P., Hermes, J.J., Barlow, B.N., Lopez, I.D., Boudreaux, T.M., Corcoran, K.A., Bell, K.J., Montgomery, M.H., Heintz, T.M., Castanheira, B.G.,

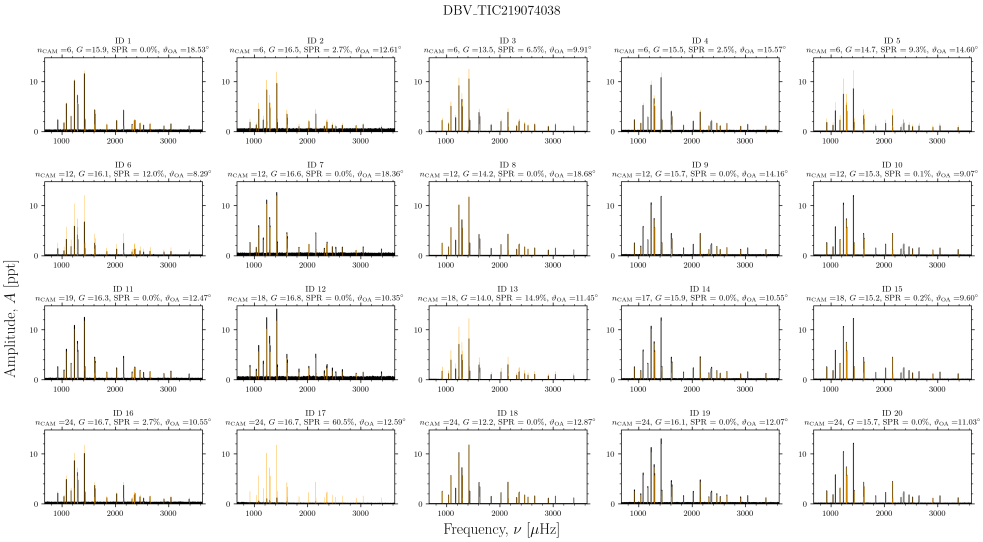


Fig. B2 Amplitude spectra of the DBV star TIC 219074038 (GD358). Same description as Fig. B1.

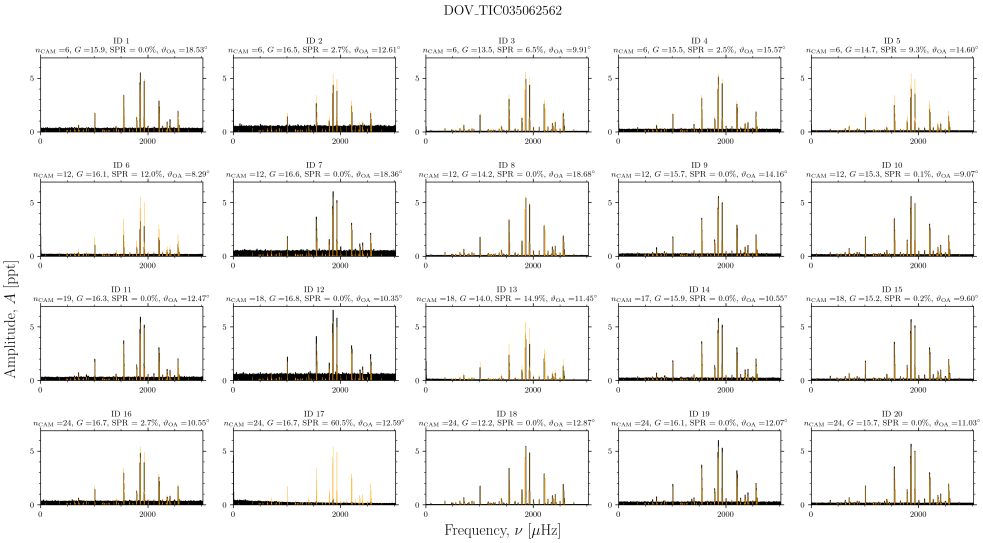


Fig. B3 Amplitude spectra of the GW vir star TIC 035062562 (PG1159-035). Same description as for Fig. B1.

Reding, J.S., Dunlap, B.H., Winget, D.E., Winget, K.I., Kuehne, J.W.: I Spy Transits and Pulsations: Empirical Variability in White Dwarfs Using Gaia and the Zwicky Transient Facility. ApJ **912**(2), 125 (2021) https://doi.org/10.3847/1538-4357/abee68 arXiv:2012.00035 [astro-ph.SR]

[6] Steen, M., Hermes, J.J., Guidry, J.A., Paiva, A., Farihi, J., Heintz, T.M., Ewing, B.B., Berry, N.: Measuring White Dwarf Variability from Sparsely Sampled Gaia DR3 Multi-epoch Photometry. ApJ **967**(2), 166 (2024) https://doi.org/10.3847/1538-4357/ad3e60 arXiv:2404.02201 [astro-ph.SR]

[7] Winget, D.E., Kepler, S.O.: Pulsating white dwarf stars and precision asteroseismology. ARA&A **46**, 157–199 (2008) https://doi.org/10.1146/annurev.astro.46.060407.145250 arXiv:0806.2573 [astro-ph]

[8] Fontaine, G., Brassard, P.: The Pulsating White Dwarf Stars. PASP **120**(872), 1043 (2008) https://doi.org/10.1086/592788

[9] Córsico, A.H., Althaus, L.G., Miller Bertolami, M.M., Kepler, S.O.: Pulsating white dwarfs: new insights. A&A Rev. **27**(1), 7 (2019) https://doi.org/10.1007/s00159-019-0118-4 arXiv:1907.00115 [astro-ph.SR]

[10] Dolez, N., Vauclair, G.: Gravity modes instability in DA white dwarfs. A&A **102**, 375–385 (1981)

[11] Dziembowski, W., Koester, D.: Excitation of gravity modes in white dwarfs with chemically stratified envelopes. A&A **97**(1), 16–26 (1981)

[12] Winget, D.E., van Horn, H.M., Tassoul, M., Fontaine, G., Hansen, C.J., Carroll, B.W.: Hydrogen-driving and the blue edge of compositionally stratified ZZ Ceti star models. ApJL **252**, 65–68 (1982) https://doi.org/10.1086/183721

[13] Starrfield, S.G., Cox, A.N., Hodson, S.W., Pesnell, W.D.: The discovery of nonradial instability strips for hot,evolved stars. ApJL **268**, 27–32 (1983) https://doi.org/10.1086/184023

[14] Starrfield, S., Cox, A.N., Kidman, R.B., Pesnell, W.D.: Nonradial instability strips based on carbon and oxygen partial ionization in hot, evolved stars. ApJ **281**, 800–810 (1984) https://doi.org/10.1086/162158

[15] Brickhill, A.J.: The pulsations of ZZ Ceti stars. III. The driving mechanism. MNRAS **251**, 673–680 (1991) https://doi.org/10.1093/mnras/251.4.673

[16] Goldreich, P., Wu, Y.: Gravity Modes in ZZ Ceti Stars. I. Quasi-adiabatic Analysis of Overstability. ApJ **511**(2), 904–915 (1999) https://doi.org/10.1086/306705 arXiv:astro-ph/9804305 [astro-ph]

[17] Luan, J., Goldreich, P.: DAVs: Red Edge and Outbursts. ApJ **863**(1), 82 (2018) https://doi.org/10.3847/1538-4357/aad0f4 arXiv:1711.06367 [astro-ph.SR]

[18] Romero, A.D., Córsico, A.H., Althaus, L.G., Kepler, S.O., Castanheira, B.G., Miller Bertolami, M.M.: Toward ensemble asteroseismology of ZZ Ceti stars with fully evolutionary models. MNRAS **420**(2), 1462–1480 (2012) https://doi.org/10.1111/j.

1365-2966.2011.20134.x arXiv:1109.6682 [astro-ph.SR]

[19] Bischoff-Kim, A., Østensen, R.H., Hermes, J.J., Provencal, J.L.: Seven-period Asteroseismic Fit of the Kepler DBV. ApJ **794**(1), 39 (2014) https://doi.org/10.1088/0004-637X/794/1/39

[20] Giammichele, N., Charpinet, S., Fontaine, G., Brassard, P., Green, E.M., Van Grootel, V., Bergeron, P., Zong, W., Dupret, M.-A.: A large oxygen-dominated core from the seismic cartography of a pulsating white dwarf. Nature **554**(7690), 73–76 (2018) https://doi.org/10.1038/nature25136

[21] Uzundag, M., De Gerónimo, F.C., Córsico, A.H., Silvotti, R., Bradley, P.A., Montgomery, M.H., Catelan, M., Toloza, O., Bell, K.J., Kepler, S.O., Althaus, L.G., Kleinman, S.J., Kilic, M., Mullally, S.E., Gänsicke, B.T., Bąkowska, K., Barber, S., Nitta, A.: Asteroseismological analysis of the polluted ZZ Ceti star G 29 - 38 with TESS. MNRAS **526**(2), 2846–2862 (2023) https://doi.org/10.1093/mnras/stad2776 arXiv:2309.04809 [astro-ph.SR]

[22] Metcalfe, T.S.: White Dwarf Asteroseismology and the $^{12}C(\alpha,\gamma)^{16}O$ Rate. ApJL **587**(1), 43–46 (2003) https://doi.org/10.1086/375044 arXiv:astro-ph/0303039 [astro-ph]

[23] Chidester, M.T., Farag, E., Timmes, F.X.: On Trapped Modes in Variable White Dwarfs as Probes of the $^{12}C(\alpha, \gamma)^{16}O$ Reaction Rate. ApJ **935**(1), 21 (2022) https://doi.org/10.3847/1538-4357/ac7ec3 arXiv:2207.02046 [astro-ph.SR]

[24] Chidester, M.T., Timmes, F.X., Farag, E.: Seismic Signatures of the $^{12}C(\alpha, \gamma)^{16}O$ Reaction Rate in White Dwarf Models with Overshooting. ApJ **954**(1), 51 (2023) https://doi.org/10.3847/1538-4357/ace620 arXiv:2307.03965 [astro-ph.SR]

[25] Caliskan, O., Uzundag, M., Kilic, M., Geronimo, F.C., Moss, A., Corsico, A.H., Parsons, S.G., Pelisoli, I., Jewett, G., Rebassa-Mansergas, A., Brown, A.J., Dhillon, V.K., Bergeron, P.: Asteroseismology of WD J004917.14-252556.81, the Most Massive Pulsating White Dwarf. arXiv e-prints, 2505–17177 (2025) arXiv:2505.17177 [astro-ph.SR]

[26] De Gerónimo, F.C., Althaus, L.G., Córsico, A.H., Romero, A.D., Kepler, S.O.: Asteroseismology of ZZ Ceti stars with fully evolutionary white dwarf models. I. The impact of the uncertainties from prior evolution on the period spectrum. A&A **599**, 21 (2017) https://doi.org/10.1051/0004-6361/201629806 arXiv:1611.10298 [astro-ph.SR]

[27] De Gerónimo, F.C., Althaus, L.G., Córsico, A.H., Romero, A.D., Kepler, S.O.: Asteroseismology of ZZ Ceti stars with full evolutionary white dwarf models. II. The impact of AGB thermal pulses on the asteroseismic inferences of ZZ Ceti stars. A&A **613**, 46 (2018) https://doi.org/10.1051/0004-6361/201731982 arXiv:1801.10589 [astro-ph.SR]

[28] Winget, D.E., van Horn, H.M., Hansen, C.J.: The nature of the ZZ Ceti oscillations - Trapped modes in compositionally stratified white dwarfs. ApJL **245**, 33–36 (1981) https://doi.org/10.1086/183516

[29] Brassard, P., Fontaine, G., Wesemael, F., Hansen, C.J.: Adiabatic Properties of Pulsating DA White Dwarfs. II. Mode Trapping in Compositionally Stratified Models. ApJS **80**, 369 (1992) https://doi.org/10.1086/191668

[30] Bradley, P.A.: Theoretical Models for Asteroseismology of DA White Dwarf Stars. ApJ **468**, 350 (1996) https://doi.org/10.1086/177696

[31] Hermes, J.J., Gänsicke, B.T., Kawaler, S.D., Greiss, S., Tremblay, P.-E., Gentile Fusillo, N.P., Raddi, R., Fanale, S.M., Bell, K.J., Dennihy, E., Fuchs, J.T., Dunlap, B.H., Clemens, J.C., Montgomery, M.H., Winget, D.E., Chote, P., Marsh, T.R., Redfield, S.: White Dwarf Rotation as a Function of Mass and a Dichotomy of Mode Line Widths: Kepler Observations of 27 Pulsating DA White Dwarfs through K2 Campaign 8. ApJS **232**(2), 23 (2017) https://doi.org/10.3847/1538-4365/aa8bb5 arXiv:1709.07004 [astro-ph.SR]

[32] Rui, N.Z., Fuller, J., Hermes, J.J.: Supersensitive Seismic Magnetometry of White Dwarfs. ApJ **981**(1), 72 (2025) https://doi.org/10.3847/1538-4357/adaf9e arXiv:2410.20557 [astro-ph.SR]

[33] Córsico, A.H., Althaus, L.G., Miller Bertolami, M.M., Romero, A.D., García-Berro, E., Isern, J., Kepler, S.O.: The rate of cooling of the pulsating white dwarf star G117-B15A: a new asteroseismological inference of the axion mass. MNRAS **424**(4), 2792–2799 (2012) https://doi.org/10.1111/j.1365-2966.2012.21401.x arXiv:1205.6180 [astro-ph.SR]

[34] Córsico, A.H., Althaus, L.G., García-Berro, E., Romero, A.D.: An independent constraint on the secular rate of variation of the gravitational constant from pulsating white dwarfs. JCAP **2013**(6), 032 (2013) https://doi.org/10.1088/1475-7516/2013/06/032 arXiv:1306.1864 [astro-ph.SR]

[35] Althaus, L.G., Camisassa, M.E., Torres, S., Battich, T., Córsico, A.H., Rebassa-Mansergas, A., Raddi, R.: Structure and evolution of ultra-massive white dwarfs in general relativity. A&A **668**, 58 (2022) https://doi.org/10.1051/0004-6361/202244604 arXiv:2208.14144 [astro-ph.SR]

[36] Althaus, L.G., Córsico, A.H., Camisassa, M.E., Torres, S., Gil-Pons, P., Rebassa-Mansergas, A., Raddi, R.: Carbon-oxygen ultra-massive white dwarfs in general relativity. MNRAS **523**(3), 4492–4503 (2023) https://doi.org/10.1093/mnras/stad1720 arXiv:2306.05251 [astro-ph.SR]

[37] Córsico, A.H., Boston, S.R., Althaus, L.G., Kilic, M., Kepler, S.O., Camisassa, M.E., Torres, S.: General relativistic pulsations of ultra-massive ZZ Ceti stars. MNRAS **524**(4), 5929–5943 (2023) https://doi.org/10.1093/mnras/stad2248 arXiv:2307.11834

[astro-ph.SR]

[38] Bédard, A.: The spectral evolution of white dwarfs: where do we stand? Ap&SS **369**(4), 43 (2024) https://doi.org/10.1007/s10509-024-04307-5 arXiv:2405.01268 [astro-ph.SR]

[39] Kepler, S.O., Pelisoli, I., Koester, D., Reindl, N., Geier, S., Romero, A.D., Ourique, G., Oliveira, C.d.P., Amaral, L.A.: White dwarf and subdwarf stars in the Sloan Digital Sky Survey Data Release 14. MNRAS **486**(2), 2169–2183 (2019) https://doi.org/10.1093/mnras/stz960 arXiv:1904.01626 [astro-ph.SR]

[40] O'Brien, M.W., Tremblay, P.-E., Klein, B.L., Koester, D., Melis, C., Bédard, A., Cukanovaite, E., Cunningham, T., Doyle, A.E., Gänsicke, B.T., Gentile Fusillo, N.P., Hollands, M.A., McCleery, J., Pelisoli, I., Toonen, S., Weinberger, A.J., Zuckerman, B.: The 40 pc sample of white dwarfs from Gaia. MNRAS **527**(3), 8687–8705 (2024) https://doi.org/10.1093/mnras/stad3773 arXiv:2312.02735 [astro-ph.SR]

[41] Kilic, M., Bergeron, P., Blouin, S., Moss, A., Brown, W.R., Bédard, A., Jewett, G., Agüeros, M.A.: The 100 pc White Dwarf Sample in the SDSS Footprint. II. A New Look at the Spectral Evolution of White Dwarfs. ApJ **979**(2), 157 (2025) https://doi.org/10.3847/1538-4357/ad9bb3 arXiv:2412.04611 [astro-ph.SR]

[42] Borucki, W.J., Koch, D., Basri, G., Batalha, N., Brown, T., Caldwell, D., Caldwell, J., Christensen-Dalsgaard, J., Cochran, W.D., DeVore, E., Dunham, E.W., Dupree, A.K., Gautier, T.N., Geary, J.C., Gilliland, R., Gould, A., Howell, S.B., Jenkins, J.M., Kondo, Y., Latham, D.W., Marcy, G.W., Meibom, S., Kjeldsen, H., Lissauer, J.J., Monet, D.G., Morrison, D., Sasselov, D., Tarter, J., Boss, A., Brownlee, D., Owen, T., Buzasi, D., Charbonneau, D., Doyle, L., Fortney, J., Ford, E.B., Holman, M.J., Seager, S., Steffen, J.H., Welsh, W.F., Rowe, J., Anderson, H., Buchhave, L., Ciardi, D., Walkowicz, L., Sherry, W., Horch, E., Isaacson, H., Everett, M.E., Fischer, D., Torres, G., Johnson, J.A., Endl, M., MacQueen, P., Bryson, S.T., Dotson, J., Haas, M., Kolodziejczak, J., Van Cleve, J., Chandrasekaran, H., Twicken, J.D., Quintana, E.V., Clarke, B.D., Allen, C., Li, J., Wu, H., Tenenbaum, P., Verner, E., Bruhweiler, F., Barnes, J., Prsa, A.: Kepler Planet-Detection Mission: Introduction and First Results. Science **327**(5968), 977 (2010) https://doi.org/10.1126/science.1185402

[43] Howell, S.B., Sobeck, C., Haas, M., Still, M., Barclay, T., Mullally, F., Troeltzsch, J., Aigrain, S., Bryson, S.T., Caldwell, D., Chaplin, W.J., Cochran, W.D., Huber, D., Marcy, G.W., Miglio, A., Najita, J.R., Smith, M., Twicken, J.D., Fortney, J.J.: The K2 Mission: Characterization and Early Results. PASP **126**(938), 398 (2014) https://doi.org/10.1086/676406 arXiv:1402.5163 [astro-ph.IM]

[44] Ricker, G.R., Winn, J.N., Vanderspek, R., Latham, D.W., Bakos, G.Á., Bean, J.L., Berta-Thompson, Z.K., Brown, T.M., Buchhave, L., Butler, N.R., Butler, R.P., Chaplin, W.J., Charbonneau, D., Christensen-Dalsgaard, J., Clampin, M., Deming, D., Doty, J., De Lee, N., Dressing, C., Dunham, E.W., Endl, M., Fressin, F., Ge, J., Henning, T., Holman, M.J., Howard, A.W., Ida, S., Jenkins, J.M., Jernigan, G., Johnson, J.A.,

Kaltenegger, L., Kawai, N., Kjeldsen, H., Laughlin, G., Levine, A.M., Lin, D., Lissauer, J.J., MacQueen, P., Marcy, G., McCullough, P.R., Morton, T.D., Narita, N., Paegert, M., Palle, E., Pepe, F., Pepper, J., Quirrenbach, A., Rinehart, S.A., Sasselov, D., Sato, B., Seager, S., Sozzetti, A., Stassun, K.G., Sullivan, P., Szentgyorgyi, A., Torres, G., Udry, S., Villasenor, J.: Transiting Exoplanet Survey Satellite (TESS). Journal of Astronomical Telescopes, Instruments, and Systems **1**, 014003 (2015) https://doi.org/10.1117/1.JATIS.1.1.014003

[45] Greiss, S., Gänsicke, B.T., Hermes, J.J., Steeghs, D., Koester, D., Ramsay, G., Barclay, T., Townsley, D.M.: KIC 11911480: the second ZZ Ceti in the Kepler field. MNRAS **438**, 3086–3092 (2014) https://doi.org/10.1093/mnras/stt2420 arXiv:1312.4541 [astro-ph.SR]

[46] Greiss, S., Gänsicke, B.T., Hermes, J.J., Giammichele, N., Fontaine, G., Koester, D., Bell, K., Breedt, E., Steeghs, D.: In: Dufour, P., Bergeron, P., Fontaine, G. (eds.) White Dwarfs in the Kepler Field - What's New? Astronomical Society of the Pacific Conference Series, vol. 493, p. 169 (2015)

[47] Greiss, S., Hermes, J.J., Gänsicke, B.T., Steeghs, D.T.H., Bell, K.J., Raddi, R., Tremblay, P.-E., Breedt, E., Ramsay, G., Koester, D., Carter, P.J., Vanderbosch, Z., Winget, D.E., Winget, K.I.: The search for ZZ Ceti stars in the original Kepler mission. MNRAS **457**, 2855–2863 (2016) https://doi.org/10.1093/mnras/stw053 arXiv:1601.01316 [astro-ph.SR]

[48] Bell, K.J., Hermes, J.J., Bischoff-Kim, A., Moorhead, S., Montgomery, M.H., Østensen, R., Castanheira, B.G., Winget, D.E.: KIC 4552982: Outbursts and Asteroseismology from the Longest Pseudo-continuous Light Curve of a ZZ Ceti. ApJ **809**, 14 (2015) https://doi.org/10.1088/0004-637X/809/1/14 arXiv:1506.07878 [astro-ph.SR]

[49] Bell, K.J., Hermes, J.J., Montgomery, M.H., Gentile Fusillo, N.P., Raddi, R., Gänsicke, B.T., Winget, D.E., Dennihy, E., Gianninas, A., Tremblay, P.-E., Chote, P., Winget, K.I.: Outbursts in Two New Cool Pulsating DA White Dwarfs. ApJ **829**, 82 (2016) https://doi.org/10.3847/0004-637X/829/2/82 arXiv:1607.01392 [astro-ph.SR]

[50] Bell, K.J., Hermes, J.J., Vanderbosch, Z., Montgomery, M.H., Winget, D.E., Dennihy, E., Fuchs, J.T., Tremblay, P.-E.: Destroying Aliases from the Ground and Space: Super-Nyquist ZZ Cetis in K2 Long Cadence Data. ApJ **851**, 24 (2017) https://doi.org/10.3847/1538-4357/aa9702 arXiv:1710.10273 [astro-ph.SR]

[51] Bell, K.J.: Pulsational oddities at the extremes of the DA white dwarf instability strip. PhD thesis, University of Texas (August 2017)

[52] Bognár, Z., Kawaler, S.D., Bell, K.J., Schrandt, C., Baran, A.S., Bradley, P.A., Hermes, J.J., Charpinet, S., Handler, G., Mullally, S.E., Murphy, S.J., Raddi, R., Sódor, Á., Tremblay, P.-E., Uzundag, M., Zong, W.: TESS first look at evolved compact pulsators. Known ZZ Ceti stars of the southern ecliptic hemisphere as

seen by TESS. A&A **638**, 82 (2020) https://doi.org/10.1051/0004-6361/202037470 arXiv:2003.11481 [astro-ph.SR]

[53] Bognár, Z., Sódor, Á., Clark, I.R., Kawaler, S.D.: ZZ Ceti stars of the southern ecliptic hemisphere re-observed by TESS. A&A **674**, 204 (2023) https://doi.org/10.1051/0004-6361/202245177 arXiv:2305.05246 [astro-ph.SR]

[54] Romero, A.D., Kepler, S.O., Hermes, J.J., Amaral, L.A., Uzundag, M., Bognár, Z., Bell, K.J., VanWyngarden, M., Baran, A., Pelisoli, I., Oliveira, G.d.R., Koester, D., Klippel, T.S., Fraga, L., Bradley, P.A., Vučković, M., Heintz, T.M., Reding, J.S., Kaiser, B.C., Charpinet, S.: Discovery of 74 new bright ZZ Ceti stars in the first three years of TESS. MNRAS **511**(2), 1574–1590 (2022) https://doi.org/10.1093/mnras/stac093 arXiv:2201.04158 [astro-ph.SR]

[55] Romero, A.D., da Rosa, G.O., Kepler, S.O., Bradley, P.A., Uzundag, M., Bell, K.J., Hermes, J.J., Lauffer, G.R.: Asteroseismology of PG 1541 + 651 and BPM 31594 with TESS. MNRAS **518**(1), 1448–1458 (2023) https://doi.org/10.1093/mnras/stac3113 arXiv:2210.15163 [astro-ph.SR]

[56] Romero, A.D., Kepler, S.O., Oliveira da Rosa, G., Hermes, J.J.: Thirty-two New Bright ZZ Ceti Stars from TESS: Adding Cycles 4 and 5. ApJ **984**(2), 112 (2025) https://doi.org/10.3847/1538-4357/adc113 arXiv:2407.07260 [astro-ph.SR]

[57] Bognár, Z., Sódor, Á.: Rotation of ZZ Ceti stars as seen by TESS. A&A **684**, 76 (2024) https://doi.org/10.1051/0004-6361/202348759 arXiv:2402.09869 [astro-ph.SR]

[58] Hermes, J.J., Montgomery, M.H., Winget, D.E., Brown, W.R., Kilic, M., Kenyon, S.J.: SDSS J184037.78+642312.3: The First Pulsating Extremely Low Mass White Dwarf. ApJL **750**(2), 28 (2012) https://doi.org/10.1088/2041-8205/750/2/L28 arXiv:1204.1338 [astro-ph.SR]

[59] Kilic, M., Hermes, J.J., Gianninas, A., Brown, W.R.: PSR J1738+0333: the first millisecond pulsar + pulsating white dwarf binary. MNRAS **446**, 26–30 (2015) https://doi.org/10.1093/mnrasl/slu152 arXiv:1410.4898 [astro-ph.SR]

[60] Althaus, L.G., Miller Bertolami, M.M., Córsico, A.H.: New evolutionary sequences for extremely low-mass white dwarfs. Homogeneous mass and age determinations and asteroseismic prospects. A&A **557**, 19 (2013) https://doi.org/10.1051/0004-6361/201321868 arXiv:1307.1882 [astro-ph.SR]

[61] Córsico, A.H., Althaus, L.G.: Pulsating low-mass white dwarfs in the frame of new evolutionary sequences. I. Adiabatic properties. A&A **569**, 106 (2014) https://doi.org/10.1051/0004-6361/201424352 arXiv:1408.6708 [astro-ph.SR]

[62] Córsico, A.H., Althaus, L.G.: Short-period g-mode Pulsations in Low-mass White Dwarfs Triggered by H-shell Burning. ApJL **793**(1), 17 (2014) https://doi.org/10.1088/2041-8205/793/1/L17 arXiv:1408.6724 [astro-ph.SR]

[63] Córsico, A.H., Althaus, L.G.: Pulsating low-mass white dwarfs in the frame of new evolutionary sequences. II. Nonadiabatic analysis. A&A **585**, 1 (2016) https://doi.org/10.1051/0004-6361/201527162 arXiv:1510.00645 [astro-ph.SR]

[64] Calcaferro, L.M., Córsico, A.H., Althaus, L.G.: Pulsating low-mass white dwarfs in the frame of new evolutionary sequences. IV. The secular rate of period change. A&A **600**, 73 (2017) https://doi.org/10.1051/0004-6361/201630376 arXiv:1701.08880 [astro-ph.SR]

[65] Calcaferro, L.M., Córsico, A.H., Althaus, L.G.: Pulsating low-mass white dwarfs in the frame of new evolutionary sequences. V. Asteroseismology of ELMV white dwarf stars. A&A **607**, 33 (2017) https://doi.org/10.1051/0004-6361/201731230 arXiv:1708.00482 [astro-ph.SR]

[66] Calcaferro, L.M., Córsico, A.H., Althaus, L.G., Romero, A.D., Kepler, S.O.: Pulsating low-mass white dwarfs in the frame of new evolutionary sequences. VI. Thin H-envelope sequences and asteroseismology of ELMV stars revisited. A&A **620**, 196 (2018) https://doi.org/10.1051/0004-6361/201833781 arXiv:1810.11502 [astro-ph.SR]

[67] Althaus, L.G., Calcaferro, L.M., Córsico, A.H., Brown, W.R.: Post-common envelope evolution of helium-core white dwarfs. A&A **699**, 280 (2025) https://doi.org/10.1051/0004-6361/202554891

[68] Lopez, I.D., Hermes, J.J., Calcaferro, L.M., Bell, K.J., Samuels, A., Vanderbosch, Z.P., Córsico, A.H., Istrate, A.G.: Discovery, TESS Characterization, and Modeling of Pulsations in the Extremely Low-mass White Dwarf GD 278. ApJ **922**(2), 220 (2021) https://doi.org/10.3847/1538-4357/ac2d28 arXiv:2110.02230 [astro-ph.SR]

[69] Calcaferro, L.M., Córsico, A.H., Althaus, L.G., Lopez, I.D., Hermes, J.J.: Exploring the internal rotation of the extremely low-mass He-core white dwarf GD 278 with TESS asteroseismology. A&A **673**, 135 (2023) https://doi.org/10.1051/0004-6361/202346007 arXiv:2303.15962 [astro-ph.SR]

[70] Kurtz, D.W., Shibahashi, H., Dhillon, V.S., Marsh, T.R., Littlefair, S.P., Copperwheat, C.M., Gänsicke, B.T., Parsons, S.G.: Hot DAVs: a probable new class of pulsating white dwarf stars. MNRAS **432**(2), 1632–1639 (2013) https://doi.org/10.1093/mnras/stt585

[71] Romero, A.D., Antunes Amaral, L., Kepler, S.O., Fraga, L., Kurtz, D., Shibahashi, H.: Pulsation in the white dwarf HE 1017-1352: confirmation of the class of hot DAV stars. MNRAS **497**(1), 24–29 (2020) https://doi.org/10.1093/mnrasl/slaa106 arXiv:2006.01008 [astro-ph.SR]

[72] Shibahashi, H.: The DB gap and pulsations of white dwarfs. In: Alecian, G., Richard, O., Vauclair, S. (eds.) EAS Publications Series. EAS Publications Series, vol. 17, pp. 143–148 (2005). https://doi.org/10.1051/eas:2005108

[73] Shibahashi, H.: The DB Gap and Pulsations of White Dwarfs. In: Stancliffe, R.J., Houdek, G., Martin, R.G., Tout, C.A. (eds.) Unsolved Problems in Stellar Physics: A Conference in Honor of Douglas Gough. American Institute of Physics Conference Series, vol. 948, pp. 35–42. AIP, ??? (2007). https://doi.org/10.1063/1.2818994

[74] Althaus, L.G., Córsico, A.H., Uzundag, M., Vučković, M., Baran, A.S., Bell, K.J., Camisassa, M.E., Calcaferro, L.M., De Gerónimo, F.C., Kepler, S.O., Silvotti, R.: About the existence of warm H-rich pulsating white dwarfs. A&A **633**, 20 (2020) https://doi.org/10.1051/0004-6361/201936346 arXiv:1911.02442 [astro-ph.SR]

[75] Koester, D., Kepler, S.O.: DB white dwarfs in the Sloan Digital Sky Survey data release 10 and 12. A&A **583**, 86 (2015) https://doi.org/10.1051/0004-6361/201527169 arXiv:1509.08244 [astro-ph.SR]

[76] Sowicka, P., Handler, G., Jones, D., Caldwell, J.A.R., van Wyk, F., Paunzen, E., Bąkowska, K., Peralta de Arriba, L., Suárez-Andrés, L., Werner, K., Karjalainen, M., Holdsworth, D.L.: The GW Vir Instability Strip in Light of New Observations of PG 1159 Stars: Discovery of Pulsations in the Central Star of A72 and Variability of RX J0122.9-7521. ApJS **269**(1), 32 (2023) https://doi.org/10.3847/1538-4365/acfbe4 arXiv:2309.16537 [astro-ph.SR]

[77] Vanderbosch, Z.P., Hermes, J.J., Winget, D.E., Montgomery, M.H., Bell, K.J., Nitta, A., Kepler, S.O.: The Pulsating Helium-atmosphere White Dwarfs. I. New DBVs from the Sloan Digital Sky Survey. ApJ **927**(2), 158 (2022) https://doi.org/10.3847/1538-4357/ac4caf arXiv:2201.09893 [astro-ph.SR]

[78] Córsico, A.H., Uzundag, M., Kepler, S.O., Althaus, L.G., Silvotti, R., Baran, A.S., Vučković, M., Werner, K., Bell, K.J., Higgins, M.: Pulsating hydrogen-deficient white dwarfs and pre-white dwarfs observed with TESS. I. Asteroseismology of the GW Vir stars RX J2117+3412, HS 2324+3944, NGC 6905, NGC 1501, NGC 2371, and K 1-16. A&A **645**, 117 (2021) https://doi.org/10.1051/0004-6361/202039202 arXiv:2011.03629 [astro-ph.SR]

[79] Uzundag, M., Córsico, A.H., Kepler, S.O., Althaus, L.G., Werner, K., Reindl, N., Bell, K.J., Higgins, M., da Rosa, G.O., Vučković, M., Istrate, A.: Pulsating hydrogen-deficient white dwarfs and pre-white dwarfs observed with TESS. II. Discovery of two new GW Vir stars: TIC 333432673 and TIC 095332541. A&A **655**, 27 (2021) https://doi.org/10.1051/0004-6361/202141253

[80] Córsico, A.H., Uzundag, M., Kepler, S.O., Silvotti, R., Althaus, L.G., Koester, D., Baran, A.S., Bell, K.J., Bischoff-Kim, A., Hermes, J.J., Kawaler, S.D., Provencal, J.L., Winget, D.E., Montgomery, M.H., Bradley, P.A., Kleinman, S.J., Nitta, A.: Pulsating hydrogen-deficient white dwarfs and pre-white dwarfs observed with TESS. III. Asteroseismology of the DBV star GD 358. A&A **659**, 30 (2022) https://doi.org/10.1051/0004-6361/202142153 arXiv:2111.15551 [astro-ph.SR]

[81] Uzundag, M., Córsico, A.H., Kepler, S.O., Althaus, L.G., Werner, K., Reindl,

N., Vučković, M.: Pulsating hydrogen-deficient white dwarfs and pre-white dwarfs observed with TESS - IV. Discovery of two new GW Vir stars: TIC 0403800675 and TIC 1989122424. MNRAS **513**(2), 2285–2291 (2022) https://doi.org/10.1093/mnras/stac1027 arXiv:2204.02501 [astro-ph.SR]

[82] Oliveira da Rosa, G., Kepler, S.O., Córsico, A.H., Costa, J.E.S., Hermes, J.J., Kawaler, S.D., Bell, K.J., Montgomery, M.H., Provencal, J.L., Winget, D.E., Handler, G., Dunlap, B., Clemens, J.C., Uzundag, M.: Kepler and TESS Observations of PG 1159-035. ApJ **936**(2), 187 (2022) https://doi.org/10.3847/1538-4357/ac8871 arXiv:2208.04791 [astro-ph.SR]

[83] Córsico, A.H., Uzundag, M., Kepler, S.O., Althaus, L.G., Silvotti, R., Bradley, P.A., Baran, A.S., Koester, D., Bell, K.J., Romero, A.D., Hermes, J.J., Gentile Fusillo, N.P.: Pulsating hydrogen-deficient white dwarfs and pre-white dwarfs observed with TESS. V. Discovery of two new DBV pulsators, WDJ152738.4−450207.4 and WD 1708−871, and asteroseismology of the already known DBV stars PG 1351+489, EC 20058−5234, and EC 04207−4748. A&A **668**, 161 (2022) https://doi.org/10.1051/0004-6361/202244198 arXiv:2210.05486 [astro-ph.SR]

[84] Calcaferro, L.M., Sowicka, P., Uzundag, M., Córsico, A.H., Kepler, S.O., Bell, K.J., Althaus, L.G., Handler, G., Kawaler, S.D., Werner, K.: Pulsating hydrogen-deficient white dwarfs and pre-white dwarfs observed with TESS. VI. Asteroseismology of the GW Vir-type central star of the Planetary Nebula NGC 246. A&A **686**, 140 (2024) https://doi.org/10.1051/0004-6361/202349103 arXiv:2402.16642 [astro-ph.SR]

[85] Tkachenko, A., Aerts, C., Jannsen, N.: Complementary Science program of the PLATO mission. In: EAS2024, European Astronomical Society Annual Meeting, p. 871 (2024)

[86] Aerts, C., Tkachenko, A.: Asteroseismic modelling of fast rotators and its opportunities for astrophysics. A&A **692**, 1 (2024) https://doi.org/10.1051/0004-6361/202348575 arXiv:2311.08453 [astro-ph.SR]

[87] Heras, A.M.: PLATO data products, access, and Guest Observer Programme. In: EAS2024, European Astronomical Society Annual Meeting, p. 2579 (2024)

[88] Werner, K., Herwig, F.: The Elemental Abundances in Bare Planetary Nebula Central Stars and the Shell Burning in AGB Stars. PASP **118**(840), 183–204 (2006) https://doi.org/10.1086/500443 arXiv:astro-ph/0512320 [astro-ph]

[89] Córsico, A.H., Althaus, L.G.: The Impact of Breathing Pulses during Core Helium Burning on the Core Chemical Structure and Pulsations of Hydrogen-rich Atmosphere White Dwarfs. ApJ **964**(1), 30 (2024) https://doi.org/10.3847/1538-4357/ad27d9 arXiv:2402.03490 [astro-ph.SR]

[90] Hollands, M.A., Tremblay, P.-E., Gänsicke, B.T., Camisassa, M.E., Koester, D., Aungwerojwit, A., Chote, P., Córsico, A.H., Dhillon, V.S., Gentile-Fusillo, N.P., Hoskin,

M.J., Izquierdo, P., Marsh, T.R., Steeghs, D.: An ultra-massive white dwarf with a mixed hydrogen-carbon atmosphere as a likely merger remnant. Nature Astronomy **4**, 663–669 (2020) https://doi.org/10.1038/s41550-020-1028-0 arXiv:2003.00028 [astro-ph.SR]

[91] Quirion, P.-O., Fontaine, G., Brassard, P.: Mapping the Instability Domains of GW Vir Stars in the Effective Temperature-Surface Gravity Diagram. ApJS **171**(1), 219–248 (2007) https://doi.org/10.1086/513870

[92] Córsico, A.H., Althaus, L.G., Kepler, S.O., Costa, J.E.S., Miller Bertolami, M.M.: Asteroseismological measurements on PG 1159-035, the prototype of the GW Virginis variable stars. A&A **478**(3), 869–881 (2008) https://doi.org/10.1051/0004-6361:20078646 arXiv:0712.0795 [astro-ph]

[93] Costa, J.E.S., Kepler, S.O.: The temporal changes of the pulsational periods of the pre-white dwarf PG 1159-035. A&A **489**(3), 1225–1232 (2008) https://doi.org/10.1051/0004-6361:20079118 arXiv:0807.5137 [astro-ph]

[94] Kepler, S.O., Nather, R.E., Winget, D.E., Nitta, A., Kleinman, S.J., Metcalfe, T., Sekiguchi, K., Jiang, X., Sullivan, D., Sullivan, T., Janulis, R., Meistas, E., Kalytis, R., Krzesinski, J., Ogoza, W., Zola, S., O'Donoghue, D., Romero-Colmenero, E., Martinez, P., Dreizler, S., Deetjen, J., Nagel, T., Schuh, S.L., Vauclair, G., Ning, F.J., Chevreton, M., Solheim, J.-E., Gonzalez Perez, J.M., Johannessen, F., Kanaan, A., Costa, J.E., Murillo Costa, A.F., Wood, M.A., Silvestri, N., Ahrens, T.J., Jones, A.K., Collins, A.E., Boyer, M., Shaw, J.S., Mukadam, A., Klumpe, E.W., Larrison, J., Kawaler, S., Riddle, R., Ulla, A., Bradley, P.: The everchanging pulsating white dwarf GD358. A&A **401**, 639–654 (2003) https://doi.org/10.1051/0004-6361:20030105 arXiv:astro-ph/0301477 [astro-ph]

[95] Castanheira, B.G., Nitta, A., Kepler, S.O., Winget, D.E., Koester, D.: HST observations of the pulsating white dwarf GD 358. A&A **432**(1), 175–179 (2005) https://doi.org/10.1051/0004-6361:20041573

[96] Provencal, J.L., Montgomery, M.H., Kanaan, A., Shipman, H.L., Childers, D., Baran, A., Kepler, S.O., Reed, M., Zhou, A., Eggen, J., Watson, T.K., Winget, D.E., Thompson, S.E., Riaz, B., Nitta, A., Kleinman, S.J., Crowe, R., Slivkoff, J., Sherard, P., Purves, N., Binder, P., Knight, R., Kim, S.-L., Chen, W.-P., Yang, M., Lin, H.C., Lin, C.C., Chen, C.W., Jiang, X.J., Sergeev, A.V., Mkrtichian, D., Andreev, M., Janulis, R., Siwak, M., Zola, S., Koziel, D., Stachowski, G., Paparo, M., Bognar, Z., Handler, G., Lorenz, D., Steininger, B., Beck, P., Nagel, T., Kusterer, D., Hoffman, A., Reiff, E., Kowalski, R., Vauclair, G., Charpinet, S., Chevreton, M., Solheim, J.E., Pakstiene, E., Fraga, L., Dalessio, J.: 2006 Whole Earth Telescope Observations of GD358: A New Look at the Prototype DBV. ApJ **693**(1), 564–585 (2009) https://doi.org/10.1088/0004-637X/693/1/564 arXiv:0811.0768 [astro-ph]

[97] Jannsen, N., Tkachenko, A., Royer, P., De Ridder, J., Seynaeve, D., Aerts, C., Aigrain, S., Plachy, E., Bodi, A., Uzundag, M., Bowman, D.M., Fritzewski, D.J., IJspeert,

L.W., Li, G., Pedersen, M.G., Vanrespaille, M., Van Reeth, T.: MOCKA – A PLATO mock asteroseismic catalogue: Simulations for gravity-mode oscillators. A&A **694**, 185 (2025) https://doi.org/10.1051/0004-6361/202452811 arXiv:2412.10508 [astro-ph.SR]

[98] Nascimbeni, V., Piotto, G., Cabrera, J., Montalto, M., Marinoni, S., Marrese, P.M., Aerts, C., Altavilla, G., Benatti, S., Börner, A., Deleuil, M., Desidera, S., Gizon, L., Goupil, M.J., Granata, V., Heras, A.M., Magrin, D., Malavolta, L., Mas-Hesse, J.M., Osborn, H.P., Pagano, I., Paproth, C., Pollacco, D., Prisinzano, L., Ragazzoni, R., Ramsay, G., Rauer, H., Tkachenko, A., Udry, S.: The PLATO field selection process: II. Characterization of LOPS2, the first long-pointing field. A&A **694**, 313 (2025) https://doi.org/10.1051/0004-6361/202452325 arXiv:2501.07687 [astro-ph.EP]

[99] Gentile Fusillo, N.P., Tremblay, P.-E., Cukanovaite, E., Vorontseva, A., Lallement, R., Hollands, M., Gänsicke, B.T., Burdge, K.B., McCleery, J., Jordan, S.: A catalogue of white dwarfs in Gaia EDR3. MNRAS **508**(3), 3877–3896 (2021) https://doi.org/10.1093/mnras/stab2672 arXiv:2106.07669 [astro-ph.SR]

[100] Pelisoli, I., Vos, J.: Gaia Data Release 2 catalogue of extremely low-mass white dwarf candidates. MNRAS **488**(2), 2892–2903 (2019) https://doi.org/10.1093/mnras/stz1876 arXiv:1907.03766 [astro-ph.SR]

[101] Bergeron, P., Dufour, P., Fontaine, G., Coutu, S., Blouin, S., Genest-Beaulieu, C., Bédard, A., Rolland, B.: On the Measurement of Fundamental Parameters of White Dwarfs in the Gaia Era. ApJ **876**(1), 67 (2019) https://doi.org/10.3847/1538-4357/ab153a arXiv:1904.02022 [astro-ph.SR]

[102] Press, W.H., Flannery, B.P., Teukolsky, S.A.: Numerical Recipes. The Art of Scientific Computing, (1986)

[103] Dufour, P., Blouin, S., Coutu, S., Fortin-Archambault, M., Thibeault, C., Bergeron, P., Fontaine, G.: The Montreal White Dwarf Database: A Tool for the Community. In: Tremblay, P.-E., Gaensicke, B., Marsh, T. (eds.) 20th European White Dwarf Workshop. Astronomical Society of the Pacific Conference Series, vol. 509, p. 3 (2017). https://doi.org/10.48550/arXiv.1610.00986

[104] Bédard, A., Bergeron, P., Brassard, P., Fontaine, G.: On the Spectral Evolution of Hot White Dwarf Stars. I. A Detailed Model Atmosphere Analysis of Hot White Dwarfs from SDSS DR12. ApJ **901**(2), 93 (2020) https://doi.org/10.3847/1538-4357/abafbe arXiv:2008.07469 [astro-ph.SR]

[105] Vincent, O., Barstow, M.A., Jordan, S., Mander, C., Bergeron, P., Dufour, P.: Classification and parameterization of a large Gaia sample of white dwarfs using XP spectra. A&A **682**, 5 (2024) https://doi.org/10.1051/0004-6361/202347694 arXiv:2308.05572 [astro-ph.SR]

[106] Koester, D., Kepler, S.O.: DB white dwarfs in the Sloan Digital Sky Survey data

release 10 and 12. A&A **583**, 86 (2015) https://doi.org/10.1051/0004-6361/201527169 arXiv:1509.08244 [astro-ph.SR]

[107] Vincent, O., Bergeron, P., Lafrenière, D.: Searching for ZZ Ceti White Dwarfs in the Gaia Survey. AJ **160**(6), 252 (2020) https://doi.org/10.3847/1538-3881/abbe20 arXiv:2010.02376 [astro-ph.SR]

[108] Castanheira, B.G., Kepler, S.O.: Seismological studies of ZZ Ceti stars - II. Application to the ZZ Ceti class. MNRAS **396**(3), 1709–1731 (2009) https://doi.org/10.1111/j.1365-2966.2009.14855.x

[109] Kilkenny, D., O'Donoghue, D., Crause, L.A., Hambly, N., MacGillivray, H.: Two new pulsating DB Stars from the EC survey, EC 04207-4748 and EC 05221-4725. MNRAS **397**(1), 453–457 (2009) https://doi.org/10.1111/j.1365-2966.2009.14966.x

[110] Higgins, M.E., Bell, K.J.: Localizing Sources of Variability in Crowded TESS Photometry. AJ **165**(4), 141 (2023) https://doi.org/10.3847/1538-3881/acb20c arXiv:2204.06020 [astro-ph.IM]

[111] Oliveira da Rosa, G., Kepler, S.O., Soethe, L.T.T., Romero, A.D., Bell, K.J.: Photometric White Dwarf Rotation. ApJ **974**(2), 314 (2024) https://doi.org/10.3847/1538-4357/ad6987 arXiv:2407.05214 [astro-ph.SR]

[112] Hernandez, M.S., Schreiber, M.R., Landstreet, J.D., Bagnulo, S., Parsons, S.G., Chavarria, M., Toloza, O., Bell, K.J.: Rotation plays a role in the generation of magnetic fields in single white dwarfs. MNRAS **528**(4), 6056–6074 (2024) https://doi.org/10.1093/mnras/stae307 arXiv:2401.15158 [astro-ph.SR]

[113] Thorstensen, J.R., Alvarado-Anderson, C.K., Burrows, A.D., Goebel-Bain, R.M., Katz, D.C.: Optical Studies of Seven Bright Southern Cataclysmic Variable Stars. AJ **166**(3), 131 (2023) https://doi.org/10.3847/1538-3881/ace7bf arXiv:2307.07630 [astro-ph.SR]

[114] Thorstensen, J.R., Fenton, W.H.: Five Dwarf Novae with Orbital Periods below Two Hours. PASP **115**(803), 37–42 (2003) https://doi.org/10.1086/345103 arXiv:astro-ph/0209172 [astro-ph]

[115] Kato, T., Santallo, R., Bolt, G., Richards, T., Nelson, P., Monard, B., Uemura, M., Kiyota, S., Stubbings, R., Pearce, A., Watanabe, T., Schmeer, P., Yamaoka, H.: Photometric study of new southern SU UMa-type dwarf novae and candidates: V877 Ara, KK Tel and PU CMa. MNRAS **339**(3), 861–871 (2003) https://doi.org/10.1046/j.1365-8711.2003.06229.x arXiv:astro-ph/0210674 [astro-ph]

[116] Warner, B., Brickhill, A.J.: Observations of rapid blue variables - XIII: Rapid pulsations in VW Hyi during outburst. MNRAS **166**, 673–681 (1974) https://doi.org/10.1093/mnras/166.3.673

[117] Kosakowski, A., Kilic, M., Brown, W.R., Gianninas, A.: The ELM Survey South. I. An Effective Search for Extremely Low Mass White Dwarfs. ApJ **894**(1), 53 (2020) https://doi.org/10.3847/1538-4357/ab8300 arXiv:2004.04202 [astro-ph.SR]

[118] Antunes Amaral, L., Vučković, M., Pelisoli, I., Istrate, A., Kepler, S.O., Hibbert, J.M.: Searching for new variable white dwarfs: The discovery of the three new pulsating and three new binary systems. A&A **694**, 246 (2025) https://doi.org/10.1051/0004-6361/202453308 arXiv:2501.09003 [astro-ph.SR]

[119] Eschen, Y.N.E., Bayliss, D., Wilson, T.G., Kunimoto, M., Pelisoli, I., Rodel, T.: Viewing the PLATO LOPS2 field through the lenses of TESS. MNRAS **535**(2), 1778–1795 (2024) https://doi.org/10.1093/mnras/stae2427 arXiv:2409.13039 [astro-ph.EP]

[120] Preval, S.P., Barstow, M.A., Bainbridge, M., Reindl, N., Ayres, T., Holberg, J.B., Barrow, J.D., Lee, C.-C., Webb, J.K., Hu, J.: A far-UV survey of three hot, metal-polluted white dwarf stars: WD0455-282, WD0621-376, and WD2211-495. MNRAS **487**(3), 3470–3487 (2019) https://doi.org/10.1093/mnras/stz1506 arXiv:1905.12350 [astro-ph.SR]

[121] Butler, R.P., Tinney, C.G., Marcy, G.W., Jones, H.R.A., Penny, A.J., Apps, K.: Two New Planets from the Anglo-Australian Planet Search. ApJ **555**(1), 410–417 (2001) https://doi.org/10.1086/321467

[122] Mugrauer, M., Neuhäuser, R., Mazeh, T.: The multiplicity of exoplanet host stars. Spectroscopic confirmation of the companions GJ 3021 B and HD 27442 B, one new planet host triple-star system, and global statistics. A&A **469**(2), 755–770 (2007) https://doi.org/10.1051/0004-6361:20065883 arXiv:astro-ph/0703795 [astro-ph]

[123] Jannsen, N., De Ridder, J., Seynaeve, D., Regibo, S., Huygen, R., Royer, P., Paproth, C., Grießbach, D., Samadi, R., Reese, D.R., Pertenais, M., Grolleau, E., Heller, R., Niemi, S.M., Cabrera, J., Börner, A., Aigrain, S., McCormac, J., Verhoeve, P., Astier, P., Kutrowski, N., Vandenbussche, B., Tkachenko, A., Aerts, C.: PlatoSim: an end-to-end PLATO camera simulator for modelling high-precision space-based photometry. A&A **681**, 18 (2024) https://doi.org/10.1051/0004-6361/202346701 arXiv:2310.06985 [astro-ph.IM]

[124] Kollmeier, J.A., Zasowski, G., Rix, H.-W., Johns, M., Anderson, S.F., Drory, N., Johnson, J.A., Pogge, R.W., Bird, J.C., Blanc, G.A., Brownstein, J.R., Crane, J.D., De Lee, N.M., Klaene, M.A., Kreckel, K., MacDonald, N., Merloni, A., Ness, M.K., O'Brien, T., Sanchez-Gallego, J.R., Sayres, C.C., Shen, Y., Thakar, A.R., Tkachenko, A., Aerts, C., Blanton, M.R., Eisenstein, D.J., Holtzman, J.A., Maoz, D., Nandra, K., Rockosi, C., Weinberg, D.H., Bovy, J., Casey, A.R., Chaname, J., Clerc, N., Conroy, C., Eracleous, M., Gänsicke, B.T., Hekker, S., Horne, K., Kauffmann, J., McQuinn, K.B.W., Pellegrini, E.W., Schinnerer, E., Schlafly, E.F., Schwope, A.D., Seibert, M., Teske, J.K., van Saders, J.L.: SDSS-V: Pioneering Panoptic Spectroscopy. arXiv e-prints, 1711–03234 (2017) https://doi.org/10.48550/arXiv.1711.03234 arXiv:1711.03234 [astro-ph.GA]

[125] de Jong, R.S., Agertz, O., Berbel, A.A., Aird, J., Alexander, D.A., Amarsi, A., Anders, F., Andrae, R., Ansarinejad, B., Ansorge, W., Antilogus, P., Anwand-Heerwart, H., Arentsen, A., Arnadottir, A., Asplund, M., Auger, M., Azais, N., Baade, D., Baker, G., Baker, S., Balbinot, E., Baldry, I.K., Banerji, M., Barden, S., Barklem, P., Barthélémy-Mazot, E., Battistini, C., Bauer, S., Bell, C.P.M., Bellido-Tirado, O., Bellstedt, S., Belokurov, V., Bensby, T., Bergemann, M., Bestenlehner, J.M., Bielby, R., Bilicki, M., Blake, C., Bland-Hawthorn, J., Boeche, C., Boland, W., Boller, T., Bongard, S., Bongiorno, A., Bonifacio, P., Boudon, D., Brooks, D., Brown, M.J.I., Brown, R., Brüggen, M., Brynnel, J., Brzeski, J., Buchert, T., Buschkamp, P., Caffau, E., Caillier, P., Carrick, J., Casagrande, L., Case, S., Casey, A., Cesarini, I., Cescutti, G., Chapuis, D., Chiappini, C., Childress, M., Christlieb, N., Church, R., Cioni, M.-R.L., Cluver, M., Colless, M., Collett, T., Comparat, J., Cooper, A., Couch, W., Courbin, F., Croom, S., Croton, D., Daguisé, E., Dalton, G., Davies, L.J.M., Davis, T., de Laverny, P., Deason, A., Dionies, F., Disseau, K., Doel, P., Döscher, D., Driver, S.P., Dwelly, T., Eckert, D., Edge, A., Edvardsson, B., Youssoufi, D.E., Elhaddad, A., Enke, H., Erfanianfar, G., Farrell, T., Fechner, T., Feiz, C., Feltzing, S., Ferreras, I., Feuerstein, D., Feuillet, D., Finoguenov, A., Ford, D., Fotopoulou, S., Fouesneau, M., Frenk, C., Frey, S., Gaessler, W., Geier, S., Gentile Fusillo, N., Gerhard, O., Giannantonio, T., Giannone, D., Gibson, B., Gillingham, P., González-Fernández, C., Gonzalez-Solares, E., Gottloeber, S., Gould, A., Grebel, E.K., Gueguen, A., Guiglion, G., Haehnelt, M., Hahn, T., Hansen, C.J., Hartman, H., Hauptner, K., Hawkins, K., Haynes, D., Haynes, R., Heiter, U., Helmi, A., Aguayo, C.H., Hewett, P., Hinton, S., Hobbs, D., Hoenig, S., Hofman, D., Hook, I., Hopgood, J., Hopkins, A., Hourihane, A., Howes, L., Howlett, C., Huet, T., Irwin, M., Iwert, O., Jablonka, P., Jahn, T., Jahnke, K., Jarno, A., Jin, S., Jofre, P., Johl, D., Jones, D., Jönsson, H., Jordan, C., Karovicova, I., Khalatyan, A., Kelz, A., Kennicutt, R., King, D., Kitaura, F., Klar, J., Klauser, U., Kneib, J.-P., Koch, A., Koposov, S., Kordopatis, G., Korn, A., Kosmalski, J., Kotak, R., Kovalev, M., Kreckel, K., Kripak, Y., Krumpe, M., Kuijken, K., Kunder, A., Kushniruk, I., Lam, M.I., Lamer, G., Laurent, F., Lawrence, J., Lehmitz, M., Lemasle, B., Lewis, J., Li, B., Lidman, C., Lind, K., Liske, J., Lizon, J.-L., Loveday, J., Ludwig, H.-G., McDermid, R.M., Maguire, K., Mainieri, V., Mali, S., Mandel, H.: 4MOST: Project overview and information for the First Call for Proposals. The Messenger **175**, 3–11 (2019) https://doi.org/10.18727/0722-6691/5117 arXiv:1903.02464 [astro-ph.IM]

[126] Ivezić, Ž., Kahn, S.M., Tyson, J.A., Abel, B., Acosta, E., Allsman, R., Alonso, D., AlSayyad, Y., Anderson, S.F., Andrew, J., Angel, J.R.P., Angeli, G.Z., Ansari, R., Antilogus, P., Araujo, C., Armstrong, R., Arndt, K.T., Astier, P., Aubourg, É., Auza, N., Axelrod, T.S., Bard, D.J., Barr, J.D., Barrau, A., Bartlett, J.G., Bauer, A.E., Bauman, B.J., Baumont, S., Bechtol, E., Bechtol, K., Becker, A.C., Becla, J., Beldica, C., Bellavia, S., Bianco, F.B., Biswas, R., Blanc, G., Blazek, J., Blandford, R.D., Bloom, J.S., Bogart, J., Bond, T.W., Booth, M.T., Borgland, A.W., Borne, K., Bosch, J.F., Boutigny, D., Brackett, C.A., Bradshaw, A., Brandt, W.N., Brown, M.E., Bullock, J.S., Burchat, P., Burke, D.L., Cagnoli, G., Calabrese, D., Callahan, S., Callen, A.L., Carlin, J.L., Carlson, E.L., Chandrasekharan, S., Charles-Emerson, G., Chesley, S., Cheu, E.C., Chiang, H.-F., Chiang, J., Chirino, C., Chow, D., Ciardi, D.R., Claver, C.F., Cohen-Tanugi, J., Cockrum, J.J., Coles, R., Connolly, A.J., Cook, K.H.,

Cooray, A., Covey, K.R., Cribbs, C., Cui, W., Cutri, R., Daly, P.N., Daniel, S.F., Daruich, F., Daubard, G., Daues, G., Dawson, W., Delgado, F., Dellapenna, A., de Peyster, R., de Val-Borro, M., Digel, S.W., Doherty, P., Dubois, R., Dubois-Felsmann, G.P., Durech, J., Economou, F., Eifler, T., Eracleous, M., Emmons, B.L., Fausti Neto, A., Ferguson, H., Figueroa, E., Fisher-Levine, M., Focke, W., Foss, M.D., Frank, J., Freemon, M.D., Gangler, E., Gawiser, E., Geary, J.C., Gee, P., Geha, M., Gessner, C.J.B., Gibson, R.R., Gilmore, D.K., Glanzman, T., Glick, W., Goldina, T., Goldstein, D.A., Goodenow, I., Graham, M.L., Gressler, W.J., Gris, P., Guy, L.P., Guyonnet, A., Haller, G., Harris, R., Hascall, P.A., Haupt, J., Hernandez, F., Herrmann, S., Hileman, E., Hoblitt, J., Hodgson, J.A., Hogan, C., Howard, J.D., Huang, D., Huffer, M.E., Ingraham, P., Innes, W.R., Jacoby, S.H., Jain, B., Jammes, F., Jee, M.J., Jenness, T., Jernigan, G., Jevremović, D., Johns, K., Johnson, A.S., Johnson, M.W.G., Jones, R.L., Juramy-Gilles, C., Jurić, M., Kalirai, J.S., Kallivayalil, N.J., Kalmbach, B., Kantor, J.P., Karst, P., Kasliwal, M.M., Kelly, H., Kessler, R., Kinnison, V., Kirkby, D., Knox, L., Kotov, I.V., Krabbendam, V.L., Krughoff, K.S., Kubánek, P., Kuczewski, J., Kulkarni, S., Ku, J., Kurita, N.R., Lage, C.S., Lambert, R., Lange, T., Langton, J.B., Le Guillou, L., Levine, D., Liang, M., Lim, K.-T., Lintott, C.J., Long, K.E., Lopez, M., Lotz, P.J., Lupton, R.H., Lust, N.B., MacArthur, L.A., Mahabal, A., Mandelbaum, R., Markiewicz, T.W., Marsh, D.S., Marshall, P.J., Marshall, S., May, M., McKercher, R., McQueen, M., Meyers, J., Migliore, M., Miller, M., Mills, D.J.: LSST: From Science Drivers to Reference Design and Anticipated Data Products. ApJ **873**(2), 111 (2019) https://doi.org/10.3847/1538-4357/ab042c arXiv:0805.2366 [astro-ph]

[127] Groot, P.J., Bloemen, S., Vreeswijk, P.M., van Roestel, J.C.J., Jonker, P.G., Nelemans, G., Klein-Wolt, M., Lepoole, R., Pieterse, D.L.A., Rodenhuis, M., Boland, W., Haverkorn, M., Aerts, C., Bakker, R., Balster, H., Bekema, M., Dijkstra, E., Dolron, P., Elswijk, E., van Elteren, A., Engels, A., Fokker, M., de Haan, M., Hahn, F., ter Horst, R., Lesman, D., Kragt, J., Morren, J., Nillissen, H., Pessemier, W., Raskin, G., de Rijke, A., Scheers, L.H.A., Schuil, M., Timmer, S.T., Antunes Amaral, L., Arancibia-Rojas, E., Arcavi, I., Blagorodnova, N., Biswas, S., Breton, R.P., Dawson, H., Dayal, P., De Wet, S., Duffy, C., Faris, S., Fausnaugh, M., Gal-Yam, A., Geier, S., Horesh, A., Johnston, C., Katusiime, G., Kelley, C., Kosakowski, A., Kupfer, T., Leloudas, G., Levan, A., Modiano, D., Mogawana, O., Munday, J., Paice, J., Patat, F., Pelisoli, I., Ramsay, G., Ranaivomanana, P.T., Ruiz-Carmona, R., Schaffenroth, V., Scaringi, S., Stoppa, F., Street, R., Tranin, H., Uzundag, M., Valenti, S., Veresvarska, M., Vučković, M., Wichern, H.C.I., Wijers, R.A.M.J., Wijnands, R.A.D., Zimmerman, E.: The BlackGEM Telescope Array. I. Overview. PASP **136**(11), 115003 (2024) https://doi.org/10.1088/1538-3873/ad8b6a arXiv:2405.18923 [astro-ph.IM]